CHAPTER TWELVE

Structural and Biophysical Methods to Analyze Clock Function and Mechanism

Martin Egli[1]
Department of Biochemistry, School of Medicine, Vanderbilt University, Nashville, Tennessee, USA
[1]Corresponding author: e-mail address: martin.egli@vanderbilt.edu

Contents

Abstract

Structural approaches have provided insight into the mechanisms of circadian clock oscillators. This review focuses upon the myriad structural methods that have been applied to the molecular architecture of cyanobacterial circadian proteins, their

Methods in Enzymology, Volume 551
ISSN 0076-6879
http://dx.doi.org/10.1016/bs.mie.2014.10.004

interactions with each other, and the mechanism of the KaiABC posttranslational oscillator. X-ray crystallography and solution NMR were deployed to gain an understanding of the three-dimensional structures of the three proteins KaiA, KaiB, and KaiC that make up the inner timer in cyanobacteria. A hybrid structural biology approach including crystallography, electron microscopy, and solution scattering has shed light on the shapes of binary and ternary Kai protein complexes. Structural studies of the cyanobacterial oscillator demonstrate both the strengths and the limitations of the divide-and-conquer strategy. Thus, investigations of complexes involving domains and/or peptides have afforded valuable information into Kai protein interactions. However, high-resolution structural data are still needed at the level of complexes between the 360-kDa KaiC hexamer that forms the heart of the clock and its KaiA and KaiB partners.

1. INTRODUCTION

Cyanobacteria are the simplest organisms known to possess a circadian clock. Initial investigations conducted some 15 years ago focused on a cluster of three genes, *kaiA*, *kaiB*, and *kaiC*, whereby *kaiA* and *kaiBC* messenger RNAs showed circadian cycling (Ishiura et al., 1998). The observations that KaiC overexpression repressed the *kaiBC* promoter and KaiA overexpression enhanced it were consistent with a transcription–translation feedback loop (TTFL) mechanism of the clock, apparently confirming the hypothesis that all biological clocks feature a TTFL at their core. This assumption was toppled by the discovery that the clock in the model organism *Synechococcus elongatus* could be reconstituted *in vitro* by mixing the KaiA, KaiB, and KaiC proteins in the presence of ATP and Mg^{2+} (Nakajima et al., 2005). Obviously, no transcription or translation is occurring in the *in vitro* system, therefore demonstrating that a TTFL as the core mechanism of circadian clocks was not obligatory. Therefore, the three proteins generate a posttranslational oscillator (PTO), with KaiC cycling through hypo and hyperphosphorylated states with a ca. 24-h period. This phosphorylation cycle controls period, formation of heteromultimeric complexes among Kai proteins and clock output signal. The latter involves the histidine kinase SasA that associates with KaiC and phosphorylates the transcription factors RpaA and RpaB that in turn modulate rhythmic expression of cyanobacterial genes in a nonpromoter-specific fashion (Markson, Piechura, Puszynska, & O'Shea, 2013).

The existence of the PTO composed of three proteins in the absence of transcription and translation provides a unique opportunity to dissect a biological clock with biochemical, biophysical, and structural means. Over the

course of the last decade, a plethora of approaches have been deployed to gain a better understanding of the structure and function of the Kai proteins and their interactions with each other over the course of the daily cycle. In particular, investigators have focused on the Kai proteins from the mesophilic *S. elongatus* and the thermophilic *Thermosynechococcus elongatus* strains for gaining a better picture of the roles of the three proteins in the PTO. KaiC is the only enzyme in the trio, acting as an ATPase, an autokinase, an autophosphatase, and a phosphotransferase. KaiC undergoes phosphorylation at two sites, Thr-432 and Ser-431 (Nishiwaki et al., 2004; Xu et al., 2004), whereby a strict order is maintained in terms of phosphorylation and dephosphorylation: $TS \rightarrow pTS \rightarrow pTpS \rightarrow TpS \rightarrow TS$ (Nishiwaki et al., 2007; Rust, Markson, Lane, Fisher, & O'Shea, 2007). KaiA stimulates phosphorylation of KaiC (Williams, Vakonakis, Golden, & LiWang, 2002; Xu, Mori, & Johnson, 2003) and KaiB antagonizes KaiA action (Kitayama, Iwasaki, Nishiwaki, & Kondo, 2003) by sequestering KaiA when KaiC is hyperphosphorylated at the interface of the KaiBC complex toward the end of the clock cycle (Brettschneider et al., 2010; Qin, Byrne, Mori, et al., 2010).

The dynamic nature of the Kai protein associations over the daily clock cycle (Mori et al., 2007) constitutes a particular challenge to the structural characterization of protein–protein interactions in the PTO. However, structural and biophysical techniques that cover the low- to high-resolution range have yielded 3D models of the individual Kai proteins in atomic detail as well as of the binary and ternary complexes at low and medium resolution (Egli, 2014; Egli & Johnson, 2013; Johnson, Egli, & Stewart, 2008; Johnson, Stewart, & Egli, 2011). This chapter provides an overview of the various techniques used to analyze structure and dynamics of Kai proteins and their complexes. Some of these same methods are being applied to the study of structure and function of mammalian circadian clock proteins, but the focus here is upon the cyanobacterial system because it is the best-characterized circadian system from the biochemical/structural perspective, and because it is the area of my expertise. I hope that describing the strengths and limitations of these methods individually will assist other researchers in their application to other clock proteins. Rather than describing individual methods in a recipe-like fashion, I have placed the emphasis on highlighting particular insights into the cyanobacterial clock that were gained from an approach and on a comparison of its advantages and limitations relative to other techniques (Table 1). At least as far as the characterization of the shape and dynamics of the PTO in broad strokes is concerned, a hybrid structural

Table 1 Strengths and limitations of individual techniques

Technique	Strengths	Limitations
PAGE (SDS/native)	SDS: assay of molecular mass, phosphorylation status Native: assay of complexes	SDS: not all proteins show mobility shifts with changes in phosphorylation Native: complexes must be very stable to withstand the long time required for electrophoretic separation
SPR	Assays of protein dynamics and/or protein interactions in solution at physiological concentrations. Can provide K_D values	Potential artifacts due to one or more of the proteins being immobilized on a surface
AUC	Accuracy; not affected by artifacts of gel filtration such as protein sticking to beads	Slow (complexes can dissociate). Sedimentation velocity is a function of both mass and shape. Requires a relatively large amount of protein
DLS	Size distribution profile of particles; determination of quaternary structures	Highly pure samples needed. Difficult to characterize polydisperse samples
TLC	Separation of small molecules such as ATP, ADP, etc	Not very quantitative unless coupled with radioactive labeling
MS	High sensitivity. Information about molecular weight, modification of proteins, e.g., phosphorylation and structure (native MS)	Not very quantitative. Sample heterogeneity sets limitations. Transfer of complexes from solution to gas phase can affect structure
FA/FRET	Assays of protein dynamics and/or protein interactions in solution at physiological concentrations. Can provide K_D values	Labeling problems: sometimes difficult to label protein(s). Protein activity affected, labeled proteins unstable?
Site-directed mutagenesis	Test hypotheses regarding the function of specific residues	Mutant proteins may be more difficult to purify.
EPMR	Information on the environment and dynamics of residues. Provides distance data (DEER)	Labeling problems: sometimes difficult to label protein(s). Protein activity affected, labeled proteins unstable?

Table 1 Strengths and limitations of individual techniques—cont'd

Technique	Strengths	Limitations
EM	Good for visualizing; can actually see proteins and their complexes. Resolutions of cryo-EM structures can extend to better than 4 Å	Static images, preparation (staining, vacuum, etc.) may significantly alter structure and/or formation of complexes
X-ray crystallography	Highest possible resolution. Accurate visualization of active sites can lead to insights into mechanism. Potential insights regarding function from structure	Requires diffraction-quality crystals. Static structure that is relatively uninformative in terms of dynamics. Trapped conformation may not be representative of active state
SAXS	Samples are in solution. Small sample size. Accurate assessment of masses, folding states, volumes, and 3D shapes. Complements crystallography and NMR	Highly sensitive to aggregation. May not provide a unique solution. Overfitting possible as a consequence of the lack of a reliable quality assessment factor
NMR	Provides conformational constraints, information on foldedness, and dynamics of proteins in solution. Chemical shift perturbation assays to detect protein–protein and protein–ligand interactions. Conditions can be readily changed	Relatively small proteins or fragments rather than full length. Results obtained with fragments may be misleading and not reflective of what the full-length protein does. Concentrations typically high, which may produce misleading results
HDX-MS	Insights into protein structural dynamics and conformational changes. Mapping solvent accessibility and protein–protein binding interfaces	Analysis of data is very tedious and time consuming
MD	Key approach for X-ray and NMR refinements, optimization of models built into EM density and SAXS envelopes. Ligand docking, homology modeling, and *ab initio* fold prediction	Simulations of large systems are prohibitively expensive (CPU time) and may limit adequate sampling of conformational states. Current force fields poorly suited to approximate quantum effects
Mathematical modeling	Provide testable predictions based on hypotheses	Sufficiently complicated models can sometimes model any phenomenon without establishing definitive tests

approach has proved to be particularly valuable. However, X-ray crystallography and solution nuclear magnetic resonance (NMR) remain the two most powerful techniques for deriving atomic-resolution structures.

2. KAI PROTEIN OVEREXPRESSION, PURIFICATION, COMPLEX FORMATION, AND ANALYSIS BY DENATURED AND NATIVE POLYACRYLAMIDE GEL ELECTROPHORESIS

2.1. Protein expression and purification

Kai proteins are expressed in *Escherichia coli* as hexahistidine-tagged (Mori et al., 2002), or GST-tagged, or (Mori et al., 2007; Nishiwaki et al., 2004) SUMO-fusion (Kim, Dong, Carruthers, Golden, & LiWang, 2008) proteins (Fig. 1). Purification entails first an affinity chromatography step and is then followed by gel filtration or ion exchange chromatography. Tags or fusions can either be removed by the appropriate proteases (e.g., enterokinase, PreScission, and Ulp1) or be retained for further experiments. In terms of the question of whether to cleave the fusion or proceed with the modified Kai protein for further studies, it is noteworthy that tags or fusion proteins may be helpful or at least not interfere with function. Thus, wild-type and mutant KaiC proteins have thus far all been crystallized with a

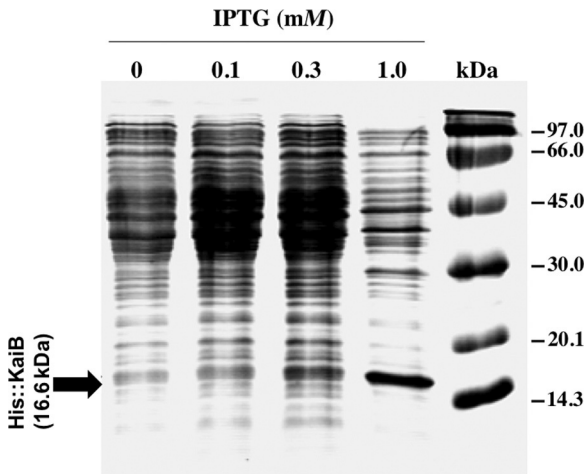

Figure 1 SDS-PAGE assay (20%) of the expression/induction of *S. elongatus* KaiB with an N-terminal $(His)_6$ tag in *E. coli* BL21 (DE3) cells as a function of isopropyl β-D-1-thiogalactopyranoside (IPTG) concentration. The KaiB monomer band is shown with an arrow, and molecular weights of marker bands are indicated on the right.

C-terminal $(His)_6$ tag (Pattanayek et al., 2009, 2004, 2011; Pattanayek, Xu, Lamichhane, Johnson, & Egli, 2014), and the tag appears not to interfere with the *in vitro* cycling reaction according to a recent report (Kitayama, Nishiwaki-Ohkawa, Sugisawa, & Kondo, 2014). In fact, even the bulky Cerulean protein fused to the C-terminal end of KaiC does not appear to distort the rhythm of the *in vitro* PTO (Ma & Ranganathan, 2012). Furthermore, FLAG-tagged Kai protein domains are routinely used for solution NMR studies (Tseng et al., 2014). However, in our hands, the C-terminal $(His)_6$ tag or Cerulean fusion do affect activity *in vitro*. And *in vivo*, there are some reports of poor rhythms with tagged proteins, while more recent papers state the opposite. Hopefully in the near future, these disparate results can be resolved among the various laboratories that study cyanobacterial clock proteins.

The identities of all purified proteins should be established by tryptic digestion in combination with electrospray ionization mass spectrometry (ESI-MS) or matrix-assisted laser desorption ionization time-of-flight mass spectrometry (MALDI-TOF MS). This is particularly important for mutant proteins of KaiC that occasionally copurify with GroEL (the two proteins have similar molecular weights (MWs), ca. 60 kDa, and form oligomers in the presence of ATP). The KaiC proteins from *S. elongatus* and *T. elongatus* also display subtle differences as a result of deviating numbers of basic and acidic residues (Pattanayek et al., 2014). Thus, the *T. elongatus* KaiC protein can be purified in the monomeric state in the absence of ATP (the same applies to a thermophilic KaiC from a source in Yellowstone Park, Mori et al., 2002), whereas KaiC from *S. elongatus* is normally purified as a hexamer with ATP bound to avoid precipitation.

2.2. Denatured and native polyacrylamide gel electrophoresis

The purity of all proteins is checked with denaturing polyacrylamide gel electrophoresis (SDS-PAGE). The KaiB protein forms a stable dimer-of-dimers in solution and in the solid state and at least the dimer band can typically be observed in SDS-PAGE along with the 13-kDa monomer. We commonly use native PAGE to assay complex formation among Kai proteins (Pattanayek et al., 2008, 2006, 2011; Qin, Byrne, Mori, et al., 2010), but have on occasion also relied on fluorescence spectroscopy to probe the interactions between Kai proteins or their peptide fragments (Pattanayek et al., 2008). Kai proteins from mesophilic and thermophilic strains may behave differently in native PAGE assays. Thus, the KaiB

proteins from *S. elongatus* and *T. elongatus* display drastically different migrations as a result of deviating numbers of acidic residues in their C-terminal tails (Pattanayek et al., 2008).

Migration in an SDS-PAGE gel cannot be taken as an absolute measure of molar mass because other factors such as charge can influence migration. This phenomenon can be useful; for example, some proteins change their charge sufficiently upon phosphorylation (or other modifications) that their migration in an SDS-PAGE gel is significantly affected. Thus, phosphoforms can be distinguished for some proteins with a simple SDS-PAGE experiment (Fig. 2). This is true for many circadian clock proteins, including KaiC, FRQ, PER, and so forth. Treatment with λ-phosphatase has been helpful with all of these clock proteins, as it converts multiple bands that represent different phosphoforms to a single band of unphosphorylated protein (Fig. 2) (e.g., Hayashi et al., 2004; Pattanayek et al., 2008; Xu et al., 2003).

Two-dimensional native and SDS-PAGE assays have been conducted with Kai clock proteins on multiple occasions (e.g., Hayashi et al., 2004 Mori et al., 2007). Thus, complexes are separated in the first dimension by native PAGE and then analyzed in terms of their composition by SDS-PAGE using staining with Coomassie blue or alternative agents. Such a protocol allows for a time-resolved analysis of the association between Kai proteins over the daily period and demonstrates the formation of KaiA:KaiC complexes during the initial phase with a concomitant increase in KaiC phosphorylation, and formation of binary KaiB:KaiC and ternary KaiA:KaiB:KaiC complexes during the dephosphorylation phase (Mori et al., 2007).

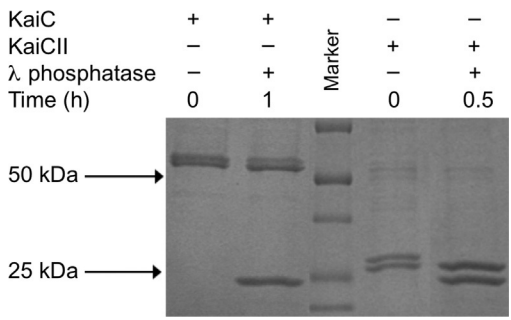

Figure 2 SDS-PAGE of phosphorylated and nonphosphorylated forms of *S. elongatus* KaiC (upper and lower band, respectively, in the 50 kDa range in the two leftmost lanes) and KaiCII, the C-terminal half of KaiC (upper and lower band, respectively, in the 25 kDa range in the two rightmost lanes). KaiC and KaiCII are gradually dephosphorylated by λ phosphatase (bottom band in lanes 2 and 5 from the left).

Related approaches for analyzing association among proteins are gel filtration chromatography in combination with SDS-PAGE or pull-down assays involving affinity tags such as $(His)_6$ or FLAG and SDS-PAGE using either standard staining techniques or immunoblotting with antibodies against individual proteins or particular tags (e.g., Chang, Kuo, Tseng, & LiWang, 2011; Hayashi et al., 2004; Kageyama et al., 2006; Pattanayek et al., 2011; Tseng et al., 2014; Villarreal et al., 2013). Native PAGE analysis of mixtures between two proteins of various ratios provides a means to measure stability parameters of their complexes, such as the dissociation constant K_D. Using this approach, the K_D for the KaiA:KaiC interaction was measured to be 152 ± 26 nM (Hayashi et al., 2004). By plotting the quotient of bound/free KaiA against bound KaiA (pmol) (Scatchard plot) based on native PAGE data, it was determined that two KaiA dimers can bind to a KaiC hexamer, although a single KaiA dimer appears to be sufficient to boost KaiC to the hyperphosphorylated state.

An alternative albeit label-free technique for quantitative measurements of biomolecular interactions is surface plasmon resonance (SPR). In this approach, one protein is immobilized on a biosensor and a solution of the prospective binding partner is channeled over the surface, whereby changes in the refractive index reflected from the biosensor are recorded. In this fashion, rate constants such as k_{on} and k_{off} as well as the dissociation constant K_D can be quantified. Kondo and coworkers used SPR with the Biacore instrument (GE Healthcare) to analyze binding of KaiA and KaiB to KaiC and found that both the association and dissociation rates for the KaiA:KaiC interaction were higher than those for KaiB:KaiC (15-and 4-fold, respectively; Kageyama et al., 2006). The values of K_D for the KaiA:KaiC and KaiB:KaiC interactions were 2.52 ± 0.46 and 8.79 ± 0.57 μM, respectively. The comparison between the affinity constants for the KaiA:KaiC complex based on SPR and native PAGE (see above) indicates that binding parameters may vary widely based on the particular techniques used.

3. ANALYTICAL ULTRACENTRIFUGATION

From the outset of investigations regarding the KaiABC PTO, the quaternary structure of individual proteins was a central concern and the use of analytical ultracentrifugation (AUC) predates by several years the discovery of the PTO. Indeed this issue has remained of crucial importance as the associations among Kai proteins and possibly their quaternary structures change over the daily cycle (Mori et al., 2007). AUC was used in

combination with native PAGE and negative stain EM (ns EM) to establish KaiC hexamer formation, and this was the first concrete indication of the homohexamer oligomeric structure of KaiC (Mori et al., 2002). Moreover, this work used AUC and EM to establish KaiC as the first circadian clock protein for which structural information about the full-length protein was visualized. By adjusting the rotor speed, AUC can assess MWs over a size range of about 100 Da–10 GDa. No sizable difference exists in terms of the amount of protein needed to carry out the individual assays. Ideally, one should use various approaches to confirm the oligomeric state of a protein. As we shall see later, the KaiB protein alone exists as a tetramer (dimer-of-dimers) in solution as well as in the crystal (Garces, Wu, Gillon, & Pai, 2004; Hitomi, Oyama, Han, Arvai, & Getzoff, 2005; Iwase et al., 2005; Pattanayek et al., 2008), but is now known to interact with the KaiC hexamer in the monomeric state (Snijder et al., 2014; Villarreal et al., 2013). An alternative method to probe the quaternary structure of proteins is gel filtration chromatography in conjunction with SDS-PAGE, as recently employed in the context of investigations directed at the KaiB:KaiC interaction (Chang, Tseng, Kuo, & LiWang, 2012). AUC is a more reliable indicator than gel filtration for quantifying the MW of a protein complex. However, it is important to note that the sedimentation velocity is a function of both molar mass and shape, and therefore, calculations of molar mass from sedimentation velocity often assume a roughly spherical shape for the protein or complex. Irrespective of the approach one may prefer it is important to bear in mind that quaternary structure can be affected by temperature and protein concentration.

4. DYNAMIC LIGHT SCATTERING

Dynamic light scattering (DLS) is a further method to assay formation of higher order structures and is exquisitely sensitive to aggregation. Parameters that can be extracted from a light scattering experiment include the translational diffusion coefficient (D_T; $[D_T] = cm^2/s$) and the hydrodynamic or Stokes radius (R_H; $[R_H] = nm$). Using DLS, it was established that KaiB forms a tetramer in solution (Hitomi et al., 2005; Fig. 3). However, DLS data that we collected for KaiBs from different cyanobacterial strains or *S. elongatus* KaiB mutants were inconclusive as to the quaternary structure of the proteins. Solutions of wild-type KaiBs from *S. elongatus* and *T. elongatus* are monodisperse and the radii consistent with tetramers that were also observed in the respective crystal structures (Pattanayek et al., 2008; Villarreal et al., 2013).

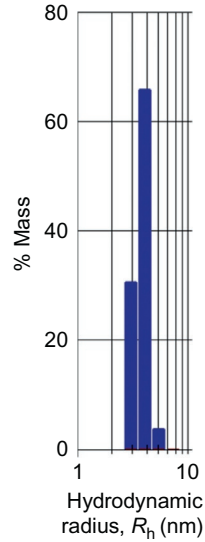

Figure 3 Dynamic light scattering of *S. elongatus* KaiB; the scattering values are the averages of 30 scans, each including 20 different time points. The translational diffusion coefficient D_T is 6.85×10^{-7} cm^2s^{-1}, the hydrodynamic radius R_h is 3.54 nm, and the mass is 65 kDa (tetramer).

However, KaiBs with up to three Asp mutations in the hydrophobic dimerization loop intended to shift the equilibrium to the monomeric state exhibit large radii/MWs that are inconsistent with monomer, dimer, or tetramer (R. Pattanayek & M. Egli, unpublished data). DLS proved to be more useful in connection with the question of the effect of oxidized plastiquinone (PQ) on the KaiA and KaiB proteins. As the cellular PQ pool increases at dusk, the compound is being transported to KaiA, causing it to aggregate and thus preventing KaiA from binding to KaiC to stimulate phosphorylation of the latter (Wood et al., 2010). DLS data acquired for solutions of KaiA in the presence of 2,5-dibromo-6-isopropyl-3-methyl-1,4-benzoquinone (DBMIB), a water-soluble PQ analog, are consistent with KaiA aggregation, whereas DBMIB has absolutely no effect on KaiB (Pattanayek, Sidiqi, & Egli, 2012).

5. THIN LAYER CHROMATOGRAPHY

Thin layer chromatography (TLC) remains a useful and inexpensive technique to screen organic chemical reactions, separate mixtures, and check purity and identity of compounds by way of a retardation factor

(R_f). The R_f of each spot can be determined by dividing the distance that a particular compound has traveled by the distance between solvent front and initial spotting site. This parameter is dependent on the TLC plate and the solvent. TLC is of little use to analyze Kai proteins and their interactions. However, a question that had remained unanswered until 2012 concerned the mechanism of the KaiC dephosphorylation reaction. In many publications, KaiC was referred to as an autokinase and autophosphatase. The latter terminology implied that the removal of phosphates from Thr-432 and Ser-431 involved a phosphatase, although the site of this activity in KaiC was unknown. To address the hypothesis that the dephosphorylation reaction possibly proceeded via the formation of ATP, i.e., in a reversal of the kinase reaction and using the same active site at subunit interfaces, we assayed the formation of radioactive ATP from [8-^{14}C]ADP with TLC (Egli et al., 2012). Indeed, polyethyleneimine cellulose TLC with 2 *M* sodium acetate solution revealed the buildup of radioactive ATP, thus supporting an ATP synthase mechanism as the basis for KaiC dephosphorylation. Formation of ATP from ADP and pThr-432/pSer-431 was subsequently also established by others using an alternative approach (Nishiwaki & Kondo, 2012).

6. MASS SPECTROMETRY

In addition to the standard use of mass spectrometry for identifying proteins based on the masses of peptide fragments from protease digests, an MS-based approach is also key for identifying posttranslational modifications in proteins, such as phosphorylation, acetylation, ubiquitination, and so forth. The two phosphorylation sites Thr-432 and Ser-431 in KaiC were recovered by nanoflow liquid chromatography-electrospray tandem MS (MS/MS), following digestion with trypsin and Asp-N (Nishiwaki et al., 2004). We found the same two sites by inspecting around threonine and serine residues difference Fourier electron density maps calculated for a partially refined model of the crystal structure of *S. elongatus* KaiC (Xu et al., 2004). Positive difference density above a certain threshold in the immediate vicinity of the side chain hydroxyl groups of either amino acid was taken as an indication of phosphorylation. Unlike the data from an MS-based analysis, crystallography provides a detailed three-dimensional map of the environment of ATP and phosphorylation sites at the subunit interface. Careful examination of the kinase active site revealed a second threonine, Thr-426, whose side chain was engaged in a H-bond to pSer-431 (Xu et al.,

2004). Subsequent structure and function investigations with KaiCs featuring mutations in the phosphorylation sites provided strong evidence that the residue at position 426 needs to be phosphorylatable and that Thr-426 is a short-lived phosphorylation site that when mutated renders the clock arrhythmic (Pattanayek et al., 2009; Xu et al., 2009). Sequential phosphorylation of KaiC, i.e., first Thr-432 and then Ser-431 followed by dephosphorylation in the same order (TS → pTS → pTpS → TpS → TS), was first established by tracking the *in vitro* cycling reaction and analyzing digested KaiC protein samples mass spectrometrically (Nishiwaki et al., 2007; Rust et al., 2007). However, with the identity of gel bands confirmed, subsequent studies analyzing the effects of mutations on the clock period *in vitro* relied on SDS-PAGE to establish the phosphorylation rhythm.

7. SITE-DIRECTED MUTAGENESIS

Mutagenesis is commonly used to study the function of genes and proteins. In the context of the cyanobacterial clock, phosphorylation site mutants of KaiC as well as KaiCs with mutations in the active site at the subunit interface have been analyzed in detail (Pattanayek et al., 2009, 2011; Xu et al., 2004, 2009). As well, KaiCs with C-terminal deletions were studied in regard to their phosphorylation states and binding to KaiA that is known to contact the C-terminal region of KaiC (Kim et al., 2008; Pattanayek et al., 2006; Vakonakis & LiWang, 2004). Nowadays kits from various manufacturers are used to introduce mutations, insertions, or deletions in a protein. Two primers, with one or both of them carrying the desired mutation(s) are annealed to the plasmid for PCR amplification. Following ligation to circularize the mutated PCR products and transformation of the resulting plasmid into *E. coli*, overexpression of mutant protein proceeds in an analogous fashion to that of wild-type protein. However, depending on the particular changes introduced into the protein, the expression efficiency may vary and it is often necessary to optimize expression parameters such as temperature and induction. Similarly, the purification protocol may have to be adapted as mutations can alter protein stability, structure, and electrostatic surface potential in addition to activity (i.e., ATPase, kinase, and ATP phosphotransferase in the case of KaiC). Whole gene synthesis offers an attractive alternative to the above mutation strategy, particularly in cases where multiple changes are introduced into a protein at distant sites. For example, one may want to produce a KaiC mutant with a C-terminal deletion as well as mutations in the phosphorylation site in the C-terminal half and mutations

in the ATPase in the N-terminal half. Rather than going through a stepwise mutation procedure, commercial custom gene synthesis and insertion into the desired expression vector may then offer a cost- and time-efficient alternative.

8. FLUORESCENCE TECHNIQUES (LABELED PROTEINS, ANISOTROPY, AND FLUORESCENCE RESONANCE ENERGY TRANSFER)

Fluorescence has become a standard method in many biologists' toolbox, especially in cell biology, where the ability to fuse genetically encoded proteins with fluorescent proteins (e.g., Green Fluorescent Protein) has revolutionized our understanding of where and how proteins act within cells. Fluorescence methods have had a similar impact in biochemistry, and in particular, the biochemistry of circadian clock proteins. One simple fluorescence application has been the labeling of FLAG-tagged KaiC proteins with fluorochromes (e.g., Alexa Fluor 532 and Cy5) and performing *in vitro* pulldowns with an anti-FLAG antibody to confirm that KaiC exchanges monomers among the KaiC hexamers in the population (Ito et al., 2007). Several groups have used the technique of fluorescence anisotropy (FA) to assess the dynamics of Kai protein complex formation and apparent dissociation constants (Qin, Byrne, Mori, et al., 2010; Tseng et al., 2014). The principle of FA in this application is that photons emitted from a fluorophore have a specific polarization with respect to the fluorochrome, and if the fluorochrome is rigidly attached to the protein, the plane of fluorescence emission will then reflect the orientation of the protein. When polarized light is used to excite a group of randomly oriented fluorophore-labeled proteins, most of the excited proteins will be those oriented within a particular range of angles to the applied polarization. If the proteins do not move, the emitted light will also be polarized within a particular range of angles to the applied excitation. If proteins can change their orientation before releasing photons as fluorescence emission (i.e., by tumbling in solution), this will reduce the magnitude of polarization of the emitted light. Larger proteins (or large protein complexes) tumble more slowly than smaller proteins (or small complexes). Therefore, anisotropy of the fluorescence signal can be used as a gauge of individual fluorophore-labeled proteins combining into a larger protein complex. This technique has been applied to the formation of KaiA:KaiC complexes with the fluorophore

attached to KaiA (Qin, Byrne, Mori, et al., 2010) and to the binding of fluorophore-labeled KaiB to the CI domain of KaiC (Tseng et al., 2014).

FA is a useful technique if the fluorophores are relatively far apart. If they are very close to one another, they can exchange energy by fluorescence resonance energy transfer (FRET). In this process, one fluorophore (the "donor") transfers its excited-state energy to another fluorophore (the "acceptor") that usually emits fluorescence of a different color. FRET efficiency depends on the spectral overlap, the relative orientation, and the distance between the donor and acceptor fluorophores. Generally, FRET occurs when the donor and acceptor are 10–100 Å apart, so it can be used to assay protein–protein proximity by attaching the donor and acceptor fluorophores to the candidate proteins. Therefore, FRET can be used as a "molecular ruler" to confirm that two proteins are interacting. In the case of circadian clock proteins, FRET was used to confirm the exchange of KaiC monomers among hexamers (Mori et al., 2007; Fig. 4). Kageyama and coworkers had previously used FLAG-tagged KaiC proteins to demonstrate that KaiC monomers appear to exchange between KaiC hexamers (Kageyama et al., 2006). However, pull-down assays of FLAG-tagged

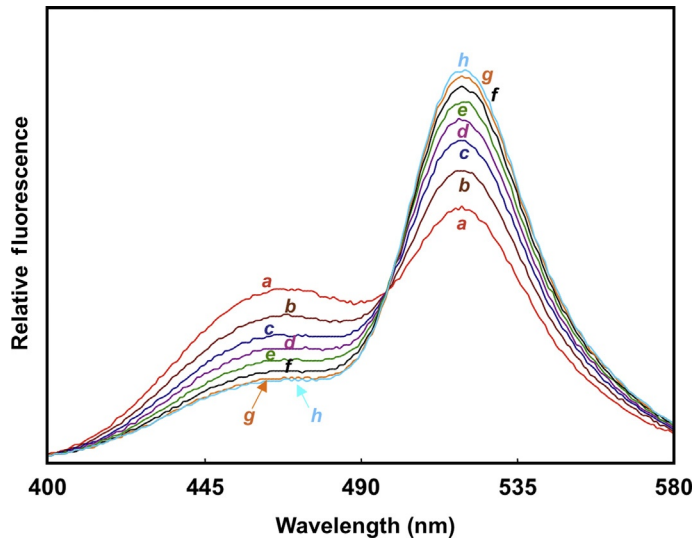

Figure 4 KaiC monomer exchange assayed by FRET. Equal populations of *S. elongatus* KaiC labeled with IAEDANS or MTSF were mixed and emission spectra of KaiC excited at 336 nm recorded at times (a) 0, (b) 0.16, (c) 0.5, (d) 1, (e) 2, (f) 4, (g) 6, and (h) 8 h after mixing at 30 °C. The decrease in fluorescence intensity at 470 nm of IAEDANS-labeled KaiC is indicative of energy transfer due to subunit shuffling between the two KaiC populations. *Adapted from Mori et al. (2007).*

proteins can suffer from differential cross-reactivity and aggregation. Therefore, we used a completely different technique to confirm KaiC monomer exchange, namely FRET (Mori et al., 2007). KaiC has three intrinsic cysteine residues that can be used for labeling with fluorophores. IAEDANS and MTSF, well-characterized FRET fluorophore partners, were used to label KaiC. One group of KaiC hexamers was labeled with IAEDANS and the other with MTSF. These groups were then mixed and incubated while monitoring the time-dependent change in quenching of IAEDANS fluorescence (indicative of FRET) in response to excitation at the excitation maximum for IAEDANS. During the incubation of the two populations of KaiC, the emission at the emission peak for IAEDANS decreased progressively (Mori et al., 2007; Fig. 4). That result indicated that monomer exchange among the two groups of KaiC had occurred, confirming the previous results that utilized pulldowns (Kageyama et al., 2006).

9. ELECTRON MICROSCOPY

Electron microscopy (EM) is a versatile technique that permits visualization of molecules and molecular assemblies with MWs >100 kDa. There is really no upper limit in terms of the size of the molecules that can be studied with EM, and improvements in detector technology now render electron crystallography a viable alternative to X-ray crystallography, as exemplified by recent EM structures of adenovirus (Reddy, Natchiar, Stewart, & Nemerow, 2010) and the ribosome (Amunts et al., 2014). The two most common approaches for analyzing macromolecular samples are ns EM and cryo-EM and both have been used for investigating the architecture of the KaiABC PTO.

9.1. Negative stain EM

For ns EM, samples are applied to a grid and stained with a solution of uranyl formate or acetate. Electron micrographs are then collected and individual particles (raw images), typically 1000s, are selected and classified. The latter procedure can be performed manually or in an automated fashion and basically entails grouping particles into classes of similar orientation by translational and rotational alignment. Averaging of such classes furnishes class sum images that exhibit an improved signal-to-noise ratio compared to raw images. Obviously, the quality of the classification is dependent on how well the alignments are done and alignment and classification steps can be repeated several times to optimize the data analysis. Next the relative

orientations of the 2D projections in the class sums have to be determined in order to produce a 3D model, whereby the latter can be used to realign the raw images. Again, this reprojection process can be repeated to optimize the computed 3D electron density map. The resolution of the final reconstruction is assessed with the Fourier shell correlation (FSC) 0.5 threshold criterion. Models of proteins or domains from X-ray or NMR structure determinations can then be built into the EM envelope.

Early studies employed ns EM to confirm the hexameric organization of *S. elongatus* KaiC (Mori et al., 2002; Fig. 5) and the overall shape of *T. elongatus* KaiC at low resolution (Hayashi et al., 2003). By correlating the 3D shape of particles from aliquots removed during the *in vitro* cycling reaction with their composition as analyzed by 2D native blue gel assay, we were able to track the appearance of Kai protein–protein complexes over the daily period (Mori et al., 2007). Overall, four classes of particles can be distinguished: KaiC hexamer, a KaiA:KaiC complex recognizable by a protrusion at one end of the KaiC barrel, a KaiB:KaiC complex with a third layer on top of the two KaiC rings (Fig. 6), and finally a ternary KaiA:KaiB:KaiC

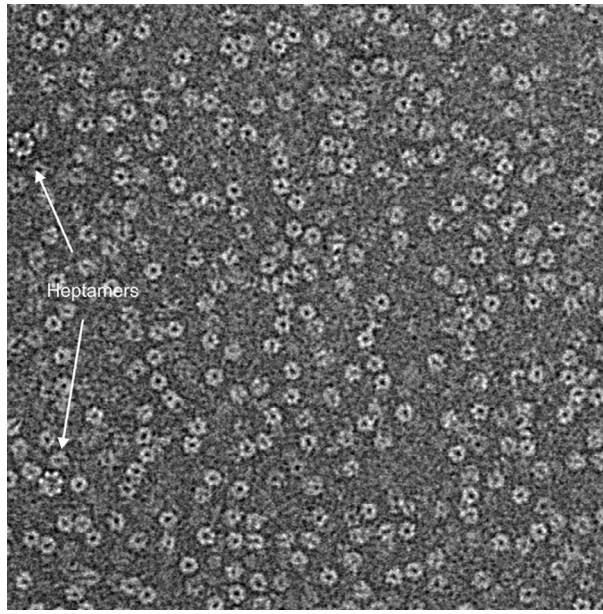

Figure 5 Negative stain electron micrograph of *S. elongatus* KaiC hexamers, viewed mostly along the central channel. Two heptameric particles are indicative of a small population of GroEL. GroEL and KaiC monomers have virtually identical molecular mass, and the former is frequently present in overexpressions of KaiC in *E. coli*.

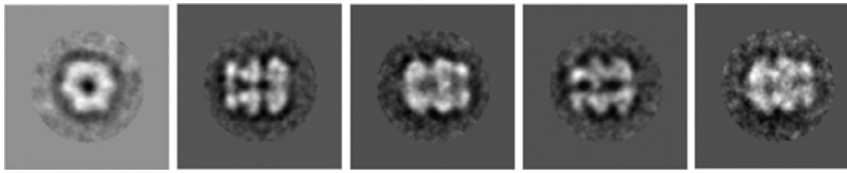

Figure 6 Class sums for the KaiB:KaiC complex from *S. elongatus* based on negative stain EM. Complex particles exhibit a characteristic three-layer shape, with the third thin layer formed by KaiB monomers.

complex with additional protrusions growing sideways from the third layer of the KaiB:KaiC complex. The KaiA:KaiC complexes from both *S. elongatus* and *T. elongatus* were studied in more detail by ns EM, and a detailed 3D reconstruction revealed two orientations of KaiA atop KaiC (Pattanayek et al., 2006). One, referred to as "tethered" exhibits a relatively large spacing between the two proteins, whereas the other, called "engaged" showed the two proteins in tight contact at the C-terminal end of KaiC. Subsequently, a model of the "engaged" complex was built into the EM electron density by taking into account the crystal structure of KaiC (Pattanayek et al., 2004), the complex based on NMR between the C-terminal domains of KaiA and C-terminal KaiC peptide (Vakonakis & LiWang, 2004), and the crystal structure of full-length KaiA (Ye, Vakonakis, Ioerger, LiWang, & Sacchettini, 2004). ns EM also provided the 3D shape of KaiA sequestered at the KaiB:KaiC interface, but the achieved resolution is too low to reveal details of the interactions between the three proteins (Pattanayek et al., 2011).

9.2. Cryo EM

Rather than by staining, samples in cryo-EM are preserved on a holey carbon grid in a frozen-hydrated state by plunging them into ethane slush cooled with liquid nitrogen. This preservation in a vitrified state prevents the collapse of samples due to dehydration upon staining. We used cryo-EM to study the *S. elongatus* KaiB:KaiC complex and an initial model showed two KaiB dimers bound to KaiC (Pattanayek et al., 2008). Because of the overall symmetry of the KaiC hexamer, it is not possible to distinguish between the N- and C-terminal hexameric rings at low resolution. Therefore, we relied on native PAGE to assay binding between separate N- and C-terminal KaiC rings and KaiB. These experiments provided support for the C-terminal but not the N-terminal hexamer interacting with KaiB. In

the model of the complex, we therefore assigned KaiB to the C-terminal end of KaiC. Subsequently, we used Ni-NTA nanogold in combination with a KaiC carrying a C-terminal $(His)_6$ tag to demonstrate that gold, His-tag, and KaiB all congregate at the C-terminal end of the KaiC hexamer (Pattanayek, Yadagirib, Ohi, & Egli, 2013). A more recent cryo-EM model of the complex between KaiB and KaiC hexamer that lacks the C-terminal 30 residues per subunit (delta-KaiC) with a resolution of 16 Å (FSC 0.5) shows six KaiB monomers forming a ring on top of the C-terminal KaiC ring, thereby covering the ATP binding clefts (Villarreal et al., 2013). Although the resolution of this $KaiC_6B_6$ model is insufficient to reveal details of the protein interactions, the binding mode suggests that KaiBs can interfere with the active site, thereby potentially limiting the kinase activity and promoting transfer of phosphates from pThr-432 and pSer-431 back to ADP. What is clear is that KaiB does not act as a competitive inhibitor of KaiA (i.e., by binding to C-terminal KaiC tails) and that at the level of the KaiC hexamer, a stable KaiB:KaiC complex exists in the absence of KaiA.

10. X-RAY CRYSTALLOGRAPHY

Single-crystal X-ray crystallography remains the most important approach for generating high-resolution 3D structural information for biomacromolecules, independent of their size. Dramatic improvements in crystallization methodology (robotics, sparse matrix crystallization screens), diffraction data collection (rapid detectors, flash freezing of crystals), phasing approaches (seleno-methionine multi- or single-wavelength anomalous dispersion, Se-Met MAD or SAD, respectively), and refinement strategies (simulated annealing, maximum likelihood analysis) render crystallography the method of choice for structure analysis at atomic resolution of proteins, nucleic acids, multiprotein complexes, and molecular machines.

Crystal structures of all three full-length Kai proteins were determined in 2004: KaiA (Ye et al., 2004) and KaiC (Pattanayek et al., 2004) from *S. elongatus* and KaiB from *Anabaena* (Garces et al., 2004). KaiA forms a domain-swapped dimer and features N-terminal bacterial response regulator-like and C-terminal four-helix bundle domains that are connected by a linker. The bundle domain forms the interface of the dyad-related homodimer and also harbors the KaiC-binding site. KaiB forms a dimer-of-dimers with subunits exhibiting a thioredoxin-like fold. All subsequent crystal structures of KaiB wild-type and mutant proteins confirmed the preference for the tetrameric quaternary

structure (Hitomi et al., 2005; Iwase et al., 2005; Pattanayek et al., 2008; Villarreal et al., 2013). A comparison of the surfaces of the KaiA and KaiB dimers revealed a striking similarity between the spacing of arginine pairs from subunits, i.e., Arg-69 residues in KaiA and Arg-23 residues in KaiB (*Anabaena* numbering; Garces et al., 2004). Thus, it seemed possible for KaiA and KaiB to compete for the same binding site on KaiC, consistent with their opposite effect on KaiC phosphorylation (Iwasaki, Nishiwaki, Kitayama, Nakajima, & Kondo, 2002; Kitayama et al., 2003). Although this scenario seemed compelling at the time, subsequent work established that KaiA and KaiB contact KaiC in different locations (Pattanayek et al., 2008, 2006; Vakonakis & LiWang, 2004). Nevertheless, the availability of structures paved the road to an interpretation of clock mutational data by mapping residues in the 3D models (Garces et al., 2004; Ye et al., 2004).

We solved the KaiC crystal structure by SAD using a tantalum bromide derivative (Pattanayek et al., 2004; Fig. 7). Annealing the crystal in the loop, i.e., by briefly diverting the coldstream and reflash cooling (Harp, Hanson, Timm, & Bunick, 1999; Fig. 8) led to a considerable improvement in the resolution limit of the diffraction data to 2.8 Å (Fig. 9). The structure revealed a homohexamer of overall dimensions $100 \times 100 \times 100$ Å, composed of two stacked rings with a constricted waist and a central channel. The N- and C-terminal domains that are the result of a gene duplication adopt a fold similar to that of recombinases (RecA) and helicases (DnaB), as anticipated from sequence considerations (Leipe, Aravind, Grishin, & Koonin, 2000). However, individual KaiC rings display a closer resemblance to F1-ATPase (Pattanayek et al., 2004), although the relationship between the KaiC homohexamer and the ATPase trimer of dimers is not apparent at the sequence level. Conversely, comparison of the KaiC rings with the structures of helicases indicates an inferior correspondence, both in terms of the diameter as well as the locations and orientations of ATP molecules.

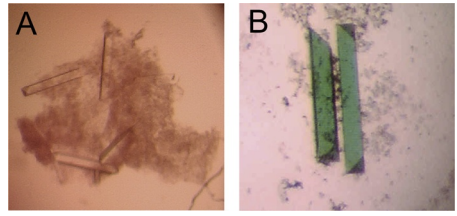

Figure 7 Crystals of (A) full-length *S. elongatus* KaiC (N1-519) with a C-terminal $(His)_6$ tag, and (B) derivatized with a tantalum bromide cluster $Ta_6Br_{12}^{2+}$ compound.

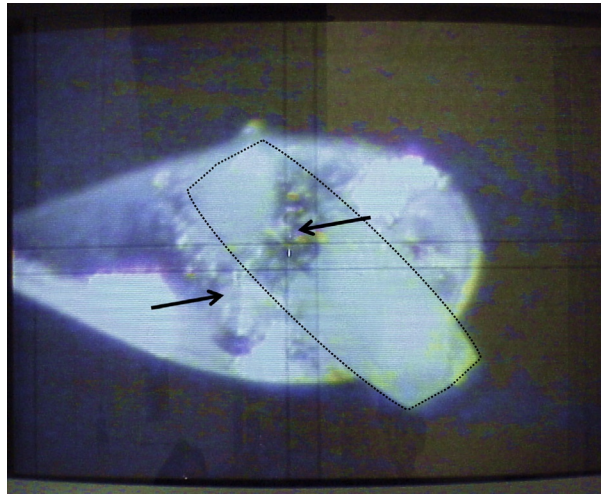

Figure 8 Annealing of a KaiC crystal (outlined with a dashed line) in the cryo-loop. The liquid N_2 stream is temporarily blocked, and the image taken from a monitor at the beam line depicts bubbling mother liquor (arrows) around the crystal as it is warming up.

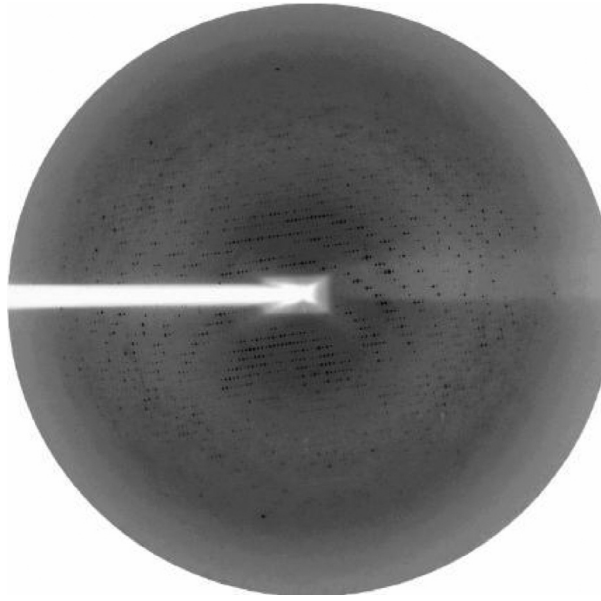

Figure 9 X-ray diffraction pattern from a KaiC crystal; the maximum resolution of the data is ca. 2.8 Å.

KaiC hexamers bind 12 ATPs, 6 each at subunit interfaces in the N- and C-terminal rings. The crystal structures of both *S. elongatus* KaiC (Pattanayek et al., 2004) and *T. elongatus* KaiC (Pattanayek et al., 2014) are trapped in the hyperphosphorylated state, and the former structure initially revealed the Thr-432 and Ser-431 phosphorylation sites in the C-terminal ring. As well, both structures were obtained for constructs with C-terminal $(His)_6$ tags, whereas constructs of full-length KaiC with His-tags or GST fusions cleaved off have thus far resisted all crystallization attempts. Subsequent structure determinations of KaiC proteins with mutations in the phosphorylation sites revealed only minor conformational changes in the overall conformations and at subunit interfaces and allowed us to identify a third short-lived phosphorylation site at Thr-426 (Pattanayek et al., 2009). Careful inspection of electron density maps allowed us to build complete or partial models of the C-terminal tails of KaiC (Pattanayek et al., 2006) that constitute the binding site for C-terminal domains of KaiA (Vakonakis & LiWang, 2004). However, to date, none of the numerous attempts to crystallize the KaiC hexamer with either KaiA or KaiB have been met with success.

X-ray crystallography is increasingly having an impact on our understanding of the mammalian and Drosophila clocks. Thus, the structures of the PAS domain fragments of the mouse PERIOD2 (mPER2; Hennig et al., 2009) and 1 and 3 proteins (mPER1, mPER3; Kucera et al., 2012) were recently reported and have revealed differences between the homodimeric interactions of the three homologues that are likely of importance in terms of their individual clock functions. Crystal structures of *Drosophila* cryptochrome (dCRY, Czarna et al., 2013; Zoltowski et al., 2011) and mouse cryptochrome 1 (mCRY1, Czarna et al., 2013) have also become available. Whereas dCRY serves as an FAD-dependent circadian photoreceptor, mCRY1 along with mCRY2 constitutes an integral part of the clock as they act as repressors of CLOCK/BMAL1-dependent transcription. A crystal structure of the latter complex revealed an asymmetric heterodimer with the basic helix-loop-helix bHLH, PAS-A, and PAS-B domains involved in three distinct dimer interfaces (Huang et al., 2012). Finally, the crystal structure of the complex between a fragment of mCRY1 encompassing the photolyase homology region and a C-terminal mPER2 fragment (Schmalen et al., 2014) provided evidence that the interaction between the two proteins is modulated by zinc binding and mCRY1 disulfide bond formation and might thus be affected by the cell's redox state.

11. SMALL-ANGLE X-RAY AND NEUTRON SCATTERING

Small-angle X-ray scattering (SAXS) has become an integral part of the so-called hybrid structural biology approach in recent years. X-ray crystallography provides a detailed picture of the 3D structure of macromolecules and their complexes, but typically allows only limited insight into dynamic aspects. SAXS affords information that is complementary to X-ray crystallography, such as on the folding and unfolding of macromolecules, aggregation, flexible domains, oligomeric state, complex formation, and 3D shape (Putnam, Hammel, Hura, & Tainer, 2007; Rambo & Tainer, 2013). The amounts of material required for solution scattering experiments are minimal compared with single-crystal X-ray crystallography and NMR solution approaches, and there are no MW limitations like those encountered in EM (lower limit) or NMR (upper limit). Unlike with crystals, the conditions in SAXS (protein concentration, ionic strength, pH, temperature, etc.) can be altered readily, allowing one to optimize various parameters in a relatively short time.

In a SAXS experiment, the scattering intensity $I(q)$ is measured as a function of the resolution or q range that is expressed as $q = (4\pi \sin\theta)/\lambda$, where 2θ is the scattering angle and λ is the radiation wavelength ($[q] = \text{Å}^{-1}$) (Fig. 10). In the so-called Guinier analysis, $\ln\{I(q)\}$ is plotted against q^2 and the resulting curve in the region closest to the zero angle is linear if there is no aggregation or other concentration-dependent phenomenon (Fig. 10). From the slope of the Guinier plot, the radius of gyration, R_G, can be extracted. R_G is the square root of the average squared distance of each scattering atom from the particle center. The Kratky plot $q^2I(q)$ versus q provides insight into the folding and flexibility of a macromolecule or macromolecular assembly. For example, a protein with a globular fold will essentially exhibit a bell-shaped curve, whereas unfolded or partially unfolded species will display a plateau or increasing $q^2I(q)$ values in the upper q range. Finally, the pairwise distribution function $P(r)$ or pair-density distribution function represents the SAXS equivalent of the Patterson function in crystallography. It can be directly computed by Fourier transforming the scattering curve $I(q)$ and provides information about the distances between electrons in the scattering sample. In theory, $P(r)$ is zero at $r = 0$ and at $r \geq D_{max}$, the maximum linear dimension of the scattering particle (Fig. 10). One of the most interesting outcomes of a SAXS experiment is the ability to carry out *ab intio* shape calculations. Because scattering curve and 3D shape of particles are related (Volkov & Svergun, 2003), it is possible to generate molecular

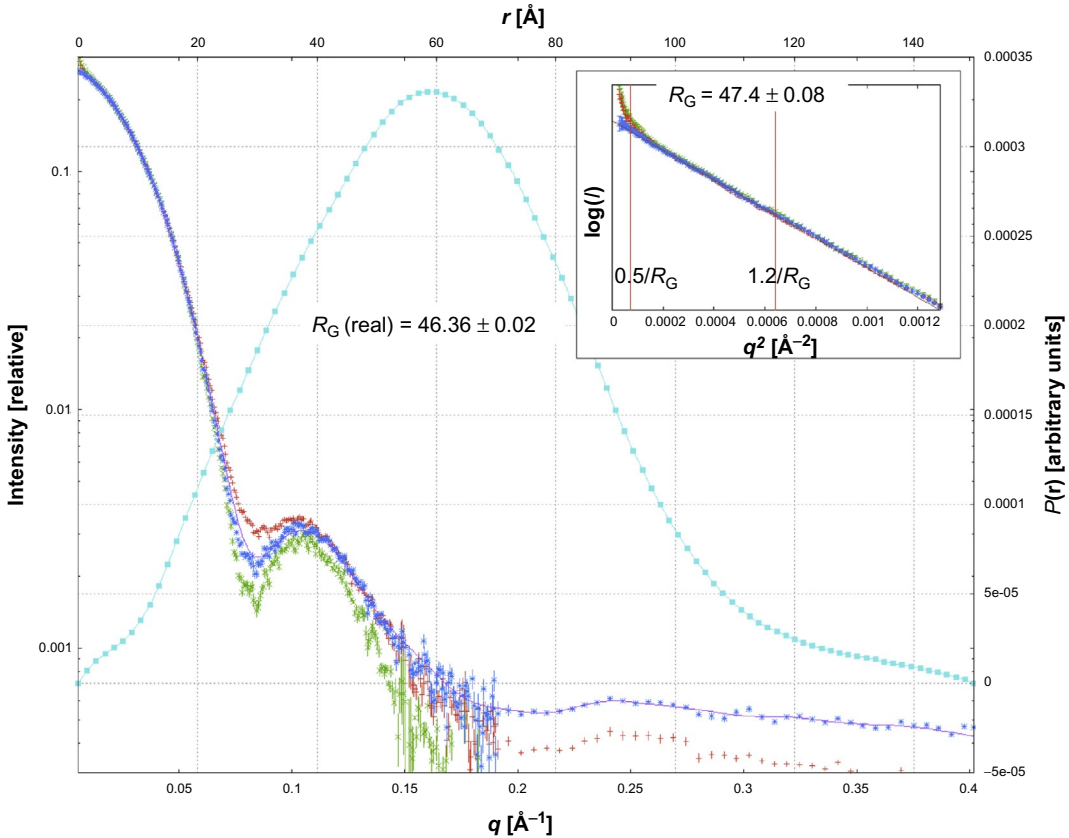

Figure 10 SAXS scattering curves $I(q)$ (red, high concentration; blue, medium concentration, and green, low concentration), pairwise function $P(r)$ (cyan), and Guinier plots (inset) for *S. elongatus* KaiC. *From Pattanayek et al. (2011).*

envelopes. Refining these entails calculating a scattering curve based on the initial model that can then be compared to the experimental curve; iterative minimization of the deviations between the experimental and theoretical scattering curves results in an improved envelope. Provided structures of the protein or the components of the macromolecular assembly under investigation are available; these can be built into the envelope and a best fit achieved with rigid-body refinement (Petoukhov & Svergun, 2005) or by applying molecular dynamics (MD) simulations (Fig. 11).

Akiyama and coworkers used SAXS with ternary KaiABC and binary KaiAC and KaiBC mixtures to chart a time course for forward scattering intensity $I(0)$ and R_G over 3 days of *in vitro* cycling (Akiyama, Nohara, Ito, & Maeda, 2008). The oscillation of intensity was in phase with that of the radius of gyration, and the latter indicated the formation of large complexes with $M_r > 470$ kDa at hours 38 and 62 and small complexes at hours 26 and 50. A SAXS-based envelope served as the basis to model KaiA dimer and KaiB tetramer at the C-terminal end of the KaiC hexamer, although no further evidence was provided to support the binding of both proteins to the same half of KaiC. We used SAXS to derive 3D models in solution of KaiA

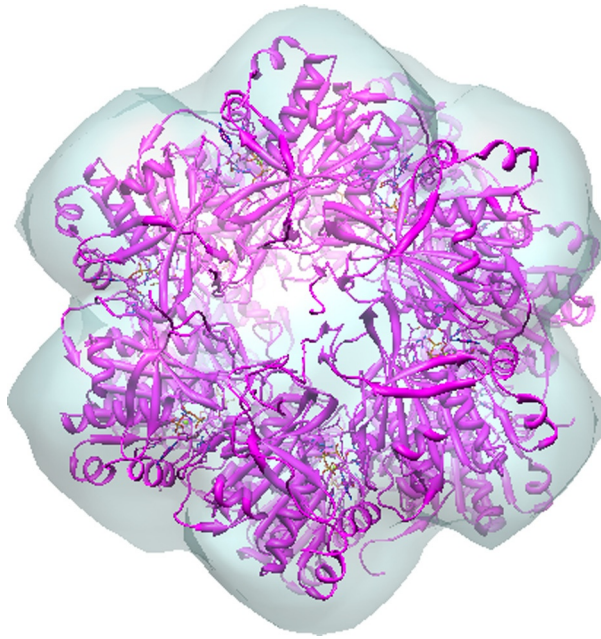

Figure 11 The crystallographic model of *S. elongatus* KaiC hexamer docked into the SAXS-based molecular envelope (using sixfold rotational symmetry constraints).

dimer, KaiB tetramer, and KaiC hexamer as well as the binary KaiAC and KaiBC complexes and, in combination with ns EM, the binary complex between KaiC and the His-kinase SasA (Pattanayek et al., 2011). Unlike EM density at low or medium resolution, the SAXS envelope for KaiC features a protrusion at one end, consistent with the presence of C-terminal tails that emerge from the dome-shaped surface near the central channel (Pattanayek et al., 2006). The SAXS envelope of the KaiBC complex was supportive of KaiB binding to the C-terminal end of KaiC because the protrusion accounting for C-terminal KaiC tails co-locates with that attributed to KaiBs. SAXS was also the key approach for tracking the expansion and contraction of the KaiC C-terminal half over the daily cycle (Murayama et al., 2011). Unlike in a crystal or on an EM grid, environments that can constrain dynamic behavior of a protein or a macromolecular assembly, such constraints are largely absent in solution and scattering provides a means to track volume changes in a particle. Accordingly, the C-terminal half of the KaiC hexamer rhythmically contracts and expands as it proceeds through various phosphorylation states, whereby the change in volume is correlated with the ATPase activity and amounts to maximal 4%.

In an attempt to study the state of KaiB (monomer, dimer, or tetramer) when bound to KaiC, we turned to small-angle neutron scattering (SANS; Jacrot, 1976). By studying the complex in mixtures of H_2O and D_2O of various ratios (contrast variation; Whitten, Cai, & Trewhella, 2008) and working with perdeuterated KaiB and hydrogenated KaiC, we intended to minimize the scatter from KaiC at the match point (ca. 40% D_2O) in order to derive a model for KaiB in combination with SAXS (R. Pattanayek, M. Egli, & W. Heller, unpublished data). However, the MWs of the two proteins differ considerably (13 kDa, KaiB monomer, vs. 360 kDa, KaiC hexamer), and the sensitivity of the approach is probably insufficient for the contribution of KaiB extracted from the overall scatter to be meaningful. Selective, partial, or completely (perdeuterated) recombinant proteins can be produced using expression systems in bacteria adapted to growth in D_2O and relying on deuterated carbon sources (Meilleur, Weiss, & Myles, 2009). The use of fully perdeuterated proteins improves the signal-to-noise ratio in neutron scattering and diffraction experiments and is essential for the study of proteins >40 kDa by solution NMR. The replacement of all hydrogen atoms by deuterium differs from the hydrogen–deuterium exchange approach (see Section 13) that is based on replacement of only a subgroup of H by D to probe protein dynamics and solvent accessibility.

12. NUCLEAR MAGNETIC RESONANCE

NMR spectroscopy in solution provides information that is complementary to that afforded by X-ray crystallography and offers insight into dynamic processes (Keeler, 2005; Wüthrich, 1986). However, compared with crystallography that can be applied to any molecular structure independent of size, NMR is generally limited to structures with MWs below 40 kDa. With specific labeling (e.g., ^{15}N, ^{13}C, ^{2}H) of particular amino acids in combination with transverse relaxation-optimized spectroscopy in two, three, or more dimensions, this limit can be pushed upward, but such experiments can become very time consuming. One of the most common NMR experiments is 2D homonuclear correlation spectroscopy. In the resulting spectra, the diagonal corresponds to the common 1D spectrum and off-diagonal peaks result from the interactions among hydrogen atoms that are relatively closely spaced. A further common type of NMR experiment for proteins is the so-called 2D heteronuclear single-quantum correlation (HSQC) spectroscopy that provides a chemical shift correlation map between directly bonded ^{1}H and nuclei such as ^{15}N or ^{13}C. Thus, each signal in a [^{15}N-^{1}H] HSQC spectrum of a protein represents a single amino acid (Fig. 12). The amount of protein necessary to conduct an NMR investigation is similar to that needed for X-ray crystallography. Unlike with the latter technique, sample conditions (e.g., temperature, and pH) can be changed quickly with NMR. However, artifacts can arise because of the use of isolated fragments or domains in order to keep the size of the molecule within a manageable range. The most time-consuming step of an NMR experiment concerns resonance assignments and the acquisition of data necessary to achieve this can take weeks or months. By comparison, X-ray diffraction data collection and processing of data are now a matter of minutes and advances in derivative preparation and phasing approaches have cut down significantly the time required to determine a crystal structure. For a more detailed comparison between the two techniques, see the overview in Egli (2010).

NMR structures of Kai protein domains emerged early on in the investigation directed at the cyanobacterial circadian clock. An initial structure of the N-terminal domain of *S. elongatus* KaiA revealed a pseudoreceiver-like fold (Williams et al., 2002). Binding assays using KaiA domains and KaiC demonstrated that the contact to the latter is exclusively established via the KaiA C-terminal domain. The NMR structure of the N-terminal

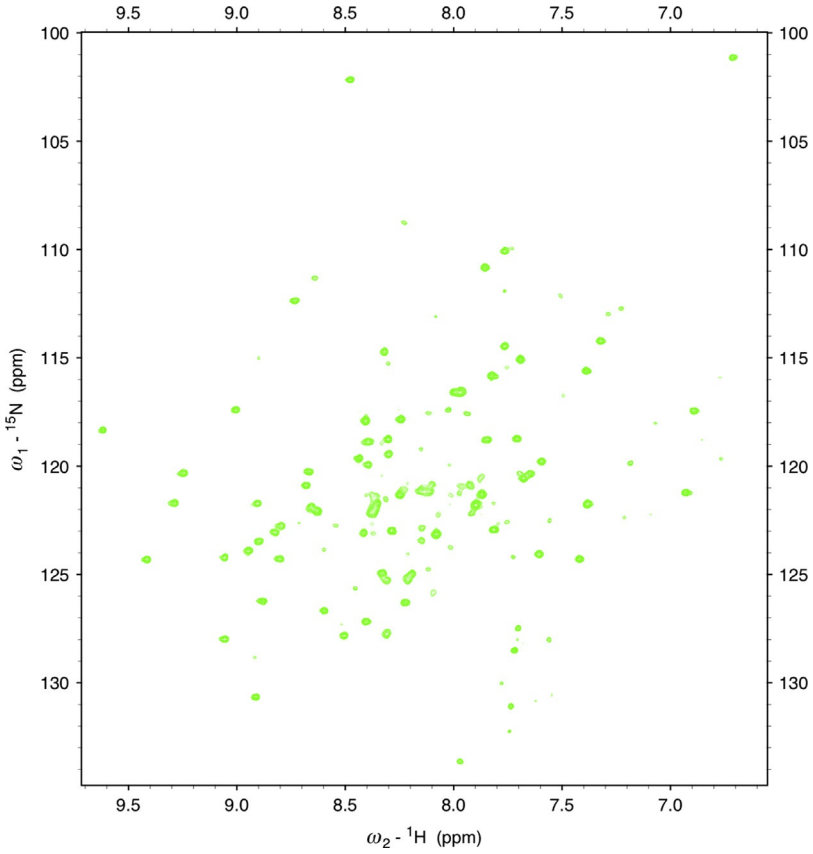

Figure 12 Two-dimensional [^{15}N-^{1}H] HSQC NMR spectrum for *S. elongatus* KaiB recorded on an 800-MHz spectrometer.

domain of the SasA histidine kinase that is involved in the clock output pathway displayed clear differences relative to the crystal structure of KaiB (Vakonakis, Klewer, Williams, Golden, & LiWang, 2004). At the sequence level, the two proteins from *S. elongatus* exhibit 28.6% identity and 55.2% similarity, and it had generally been expected that the structures would be closely related. However, no NMR solution structure of KaiB for any of the cyanobacterial strains has been reported to date. Based on the structural differences established between SasA and KaiB at the time, it appeared unlikely that the two proteins would compete for KaiC binding. More recent studies using native PAGE and ns EM have provided evidence that KaiB and SasA indeed compete for KaiC binding but exhibit divergent affinities for the central cog of the KaiABC clock (Pattanayek et al., 2011).

No consensus exists at the moment as to whether binding between KaiB (or SasA) and KaiC involves the N-terminal or C-terminal half of KaiC or both (Egli, 2014). NMR experiments provided a breakthrough in our understanding of the interaction between KaiA and KaiC. Accordingly, the C-terminal domains of KaiA dimer bind two C-terminal peptides that protrude from the surface of the KaiC hexamer (residues 488–518; *T. elongatus* protein). This binding mode results in the unraveling of so-called A-loops that rim the channel opening on the C-terminal side, a conformational change that can be transmitted to P-loop and ATP on the one hand (Kim et al., 2008) and phosphorylation sites on the other (Egli et al., 2013), consistent with the stimulation of KaiC phosphorylation by KaiA.

More recent NMR investigations of the Kai proteins concern dynamic aspects of the clock. Using separate N- and C-terminal domains from *T. elongatus* KaiC monomer, LiWang and coworkers showed that the flexibility of the C-terminal ring governs the rhythm of KaiC phosphorylation and dephosphorylation (Chang et al., 2011). Over the daily cycle, the C-terminal KaiC ring undergoes transitions from a flexible state (e.g., ST) to more rigid ones (e.g., pTpS, TpS). These changes in flexibility affect not only the interactions with KaiA and KaiB in the PTO but may also control clock output pathways (e.g., via bound SasA). Further NMR experiments with domains of KaiC monomer led to the identification of a KaiB binding site on the N-terminal half of KaiC that is apparently obscured in the KaiC hexamer (Chang et al., 2012). NMR also provides evidence that the complex between a FLAG-tagged, monomeric KaiC N-terminal domain and KaiB* (KaiB lacking its C-terminal tail and with two Tyr residues mutated to Ala in order to destabilize the dimer-of-dimers seen with wt-KaiB) is able to recruit KaiA that lacks the N-terminal domain (ΔN-KaiA) (Tseng et al., 2014). Although the observation of KaiA sequestration by monomeric fragments of KaiB and KaiC that are amenable to detailed NMR investigations alone or in complex is fascinating, it is unclear at the moment whether these structural studies can indeed capture the complexity of the interactions between full-length proteins in the ternary KaiABC complex with a MW of >500 kDa.

13. HYDROGEN–DEUTERIUM EXCHANGE

Replacement of covalently bound hydrogen by deuterium (H/D exchange or HDX) is a common approach to analyze the dynamics of

protein folding and to probe solvent accessibility and protein–protein interactions (Englander & Kallenbach, 1983; Katta & Chait, 1991; Konermann, Pan, & Liu, 2011). The exchange is also the basis for neutron crystallography and SANS. HDX combined with tryptic digestion and electrospray ionization mass spectrometry (HDX-MS) permits tracking of conformational changes and mapping of protein–protein interfaces (Mandell, Baerga-Ortiz, Falick, & Komives, 2005; Wales & Engen, 2006). Thus, sites buried upon complex formation will be less or not accessible to HDX, allowing for their subsequent identification among peptides from protein digests. HDX-MS was used to analyze the KaiB:KaiC interaction in conjunction with native MS (van Duijn, 2010) to study the KaiB quaternary structure, i.e., the distribution among monomer, dimer, and tetramer (Snijder et al., 2014). The latter investigation demonstrated that the monomeric state is predominant at lower temperature and protein concentrations. The KaiB tetramer seen in KaiB crystals (Garces et al., 2004; Hitomi et al., 2005; Iwase et al., 2005; Pattanayek et al., 2008; Villarreal et al., 2013) and in solution by SAXS (Pattanayek et al., 2011) and light scattering (Pattanayek et al., 2012) may therefore not be the form that contacts the KaiC hexamer. The HDX-MS analysis revealed limited accessibility to deuterium at subunit interfaces in the C-terminal KaiC half and at the constricted waist, consistent with binding by KaiBs on the same side as KaiA and conformational adjustments upon complex formation at the interface between the N- and C-terminal KaiC rings (Snijder et al., 2014). In combination with computational simulations of complexes with six KaiB monomers bound to either the KaiC surface at the N-or C-terminal ends and comparison of MS cross-collisional section data, it was concluded that a $KaiC_6B_6$ complex with KaiBs bound to the C-terminal ring and covering ATP binding clefts constitutes the most likely scenario. Remarkably, the stoichiometry of the KaiB:KaiC interaction, the state of KaiB as it is bound to the KaiC hexamer, and the location of KaiB binding on KaiC are fully consistent with the results from the cryo-EM analysis that also mapped six KaiB monomers to the C-terminal end of KaiC (Villarreal et al., 2013). The latter study also took into account the consequences for KaiB binding of the KaiC R468C mutation (Xu et al., 2003). This mutation results in higher affinity of KaiB for KaiC and the residue maps to the binding interface in the $KaiC_6B_6$ model proposed based on EM (Villarreal et al., 2013). One difference between the HDX-MS and cryo-EM-derived models of the KaiBC complex concerns the docking approach. The former study relied on the HADDOCK software (Dominguez, Boelens, & Bonvin, 2003) that can make use of a wide

variety of information to constrain the docking process for building models of protein–protein complexes (e.g., mutagenesis, NMR shift, and/or HDX data). The cryo-EM study used the Molecular Dynamics Flexible Fitting software (Trabuco, Villa, Schreiner, Harrison, & Schulten, 2009) to evaluate different locations and orientations of KaiB crystal structures on the KaiC hexamer within the EM-based electron density of the complex.

14. MD SIMULATIONS

MD simulations are a key component of many structural and biophysical approaches as indicated at the end of Section 13. Thus, simulated annealing can help overcome local minima in crystallographic refinement. Similarly, constrained refinement of NMR structural ensembles, SAXS-based models and cryo-EM structures often involves MD simulations. MD simulations provide detailed insight into the time-dependent behavior of a molecular system by allowing one to chart atomic fluctuations and conformational changes over a period of time (Durrant & McCammon, 2011; Fig. 13). Whereas X-ray crystallography and high-resolution cryo-EM furnish structural information at atomic resolution, MD simulations shed light on the dynamics of macromolecules and their complexes. Molecular mechanics calculations employ a force field that combines force constants, parameters (bonds, angles, torsion angles, nonbonded distances, etc.), and an energy function that together can be used to calculate the energy of a molecule. By comparison, MD simulates the atomic motions of a molecule by employing classical mechanics (Schwede & Peitsch, 2008). Thus, atoms are modeled as point charges of a certain mass that are under the influence of a force field. In subsequent steps, Newton's equation of motion is integrated at every time interval for each atom in the system to determine all their positions. Molecular motions occur at various time scales, i.e., femtoseconds to seconds (short-range motions, such as bond and angle stretching and side chain motions), nanoseconds to seconds (rigid-body motions, such as domain and subunit motions), and $>\mu$s (long-range motions, such as binding events and protein folding and unfolding). To be able to capture the short-range motions, the time step needs to be small enough; typically one time step equals 15 fs of simulation time. Similarly, to be able to observe the slower long-range motions, it is necessary to continue the simulation for as many steps as possible. However, the available computer time often sets limitations on how long a simulation can be continued for. Thus, a typical CPU consumes about 1 s of real time to compute about 1 fs of simulation

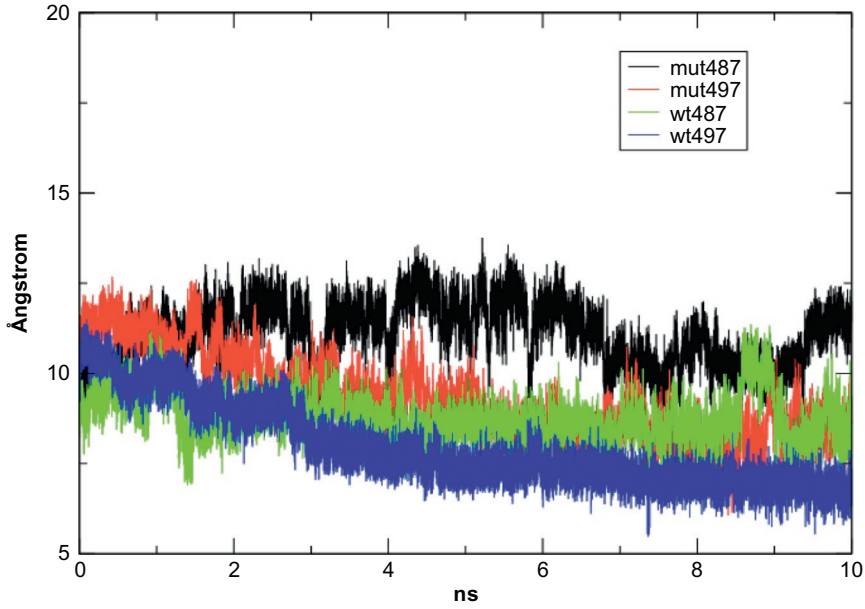

Figure 13 Variations in the distance between the Cα positions of Ser-417 and Gly-421 monitored over 10 ns of MD simulations for four KaiC hexamers: KaiC 1–497, KaiC 1–487 (lacking the so-called A-loop) and the 1–497 and 1–487 KaiCs with an additional A422V mutation. The 422-loop region encompassing residues 417–421 was hypothesized to become more flexible as a result of removal of the A-loop. Indeed, the black and green traces for the 1–487 systems without the A-loop indicate increased distance fluctuations.

time for a protein of around 200 amino acids length in a box of solvent molecules. Therefore, it follows that an MD simulations over ca. 5 ns requires about a month of computer time for a typical protein.

We carried out MD simulations for KaiC molecules with or without the A-loop regions (amino acids 487–497) to address the hypothesis that unraveling of the A-loop by KaiA (Vakonakis & LiWang, 2004) results in increased dynamics of selected regions of KaiC, consistent with stimulation of KaiC autophosphorylation by KaiA (Egli et al., 2013). We used the crystal structure of the KaiC hexamer (Pattanayek et al., 2006) as the start coordinates in combination with the AMBER software (Case et al., 2012; Götz et al., 2012), the parameters developed by Meagher and coworkers for the 12 ATP molecules (Meagher, Redman, & Carlson, 2003) and the SPC/E water model (Berendsen, Grigera, & Straatsma, 1987) with compatible ions. KaiC was hydrated with a total of 66,273 water molecules inside an orthorhombic box with an 11 Å clearance to the edges of the box.

Following minimization, the systems were equilibrated over the course of 450 ps under constant-volume conditions and finally the simulations were carried out for 25 ns, with 15 fs steps under constant pressure and no symmetry constraints applied (Egli et al., 2013). The KaiC hexamer, 6×497 amino acids (487 in the model without the A-loop) plus 12 ATPs and solvent, represents a rather large system for MD simulations, and we initially attempted to only include three subunits or limit the simulations to the C-terminal hexameric ring to conserve resources. However, neither system behaved in a stable manner and only the full hexameric particle remained stable. This is noteworthy because separate C-terminal domains do not form a stable hexamer (Hayashi, Iwase, Uzumaki, & Ishiura, 2006; Pattanayek et al., 2008). The MD simulations demonstrated that removal of the A-loop increases the root-mean-square deviation (rmsd) from the initial conformation relative to the KaiC hexamer with the A-loop present. In particular, a loop region that interacts with the A-loop and comprises residues 418–425, immediately adjacent to Thr-426, Ser-431, and Thr-432 that have all been shown to be targets of the autokinase, shows increased fluctuations upon A-loop removal (Fig. 13). As well, the absence of the A-loop leads to higher mobility of a neighboring β-strand and indirectly of the P-loop and ATP (Egli et al., 2013). Surprisingly, the lack of the A-loop region does not just cause changes in the mobility of residues that lie in the immediate vicinity of the loop, but altered fluctuations are seen also in the N-terminal ring. Overall, the outcome of the simulations is consistent with a concerted allosteric mechanism of KaiC phosphorylation that is stimulated by KaiA binding to a KaiC C-terminal tail and pulling on the A-loop from a subunit.

15. MODELING THE *IN VITRO* OSCILLATOR

Mathematical modeling can be a powerful method in conjunction with biochemical studies to provide verification of hypotheses and predictions for future experimental tests. Since the publication of the *in vitro* KaiABC rhythm, there have been many attempts to model this oscillator, e.g., reviewed in Johnson et al. (2011), and those presented in references (Byrne, 2009; Clodong et al., 2007; Emberly & Wingreen, 2006; Ito et al., 2007; Kageyama et al., 2006; Kurosawa, Aihara, & Iwasa, 2006; Li, Chen, Wang, & Wang, 2009; Li & Fang, 2007; Ma & Ranganathan, 2012; Mehra et al., 2006; Miyoshi, Nakayama, Kaizu, Iwasaki, & Tomita, 2007; Mori et al., 2007; Nagai, Terada, & Sasai, 2010; Paddock, Boyd, Adin, & Golden, 2013; Phong, Markson, Wilhoite, & Rust, 2013; Qin, Byrne,

Mori, et al., 2010; Qin, Byrne, Xu, Mori, & Johnson, 2010; Rust, Golden, & O'Shea, 2011; Takigawa-Imamura & Mochizuki, 2006; Teng, Mukherij, Moffitt, de Buyl, & O'Shea, 2013; van Zon, Lubensky, Altena, & ten Wolde, 2007; Wang, Xu, & Wang, 2009; Yang, Pando, Dong, Golden, & van Oudenaarden, 2010; Yoda, Eguchi, Terada, & Sasai, 2007; Zwicker, Lubensky, & ten Wolde, 2010). As a representative example, we proposed in 2007, a model that stochastically simulates the kinetics of KaiC hexamers and the degree of phosphorylation of each monomer in every hexamer (Mori et al., 2007). In addition to modeling the general phenomenon, that model addresses the question of how the various KaiC hexamers in a population stay in synch with each other to maintain a robust, high-amplitude oscillation *in vitro* over many days. Inspired by the experimental data of the Kondo lab (Ito et al., 2007; Kageyama et al., 2006), we incorporated phase-dependent KaiC monomer exchange as a mechanism for keeping the phosphorylation state of hexamers synchronized in the population, and our model accurately predicted the observed patterns of *in vitro* KaiC phosphorylation (Mori et al., 2007). Interestingly, monomer exchange was predicted by a modeling study before it was experimentally measured (Emberly & Wingreen, 2006) Other significant models have proposed a different mechanism for KaiC hexamer synchronization, namely synchronization by KaiA sequestration (Brettschneider et al., 2010; Clodong et al., 2007; Rust et al., 2007; van Zon et al., 2007). There is clear experimental evidence for both models (Brettschneider et al., 2010; Ito et al., 2007; Mori et al., 2007; Qin, Byrne, Mori, et al., 2010; Rust et al., 2007), and it is likely that KaiA sequestration may act in concert with monomer exchange to accomplish the synchrony of KaiC phosphorylation that enables the robust high-amplitude rhythms for many cycles *in vitro* (Ito et al., 2007). We have also generated a combined model in which monomer exchange is a mechanism for maintaining phase synchrony among KaiC hexamers while KaiA sequestration is involved in the "switch" from autokinase to autophosphatase mode (Qin, Byrne, Mori, et al., 2010). Finally, modeling studies are beginning to address how the cyanobacterial pacemaker may regulate gene expression (Paddock et al., 2013; Qin, Byrne, Xu, et al., 2010; Teng et al., 2013; Zwicker et al., 2010), metabolism (Hellweger, 2010; Rust et al., 2011), and cell division (Yang et al., 2010).

16. SUMMARY AND OUTLOOK

The KaiABC PTO has been analyzed in significant detail both at the biophysical and structural levels with a wide range of methods as indicated in

this chapter. Analyses directed at the association of Kai proteins demonstrate that the cyanobacterial inner timer is a dynamic nanomachine that exhibits changing Kai protein–protein interactions over the daily cycle (Kageyama et al., 2006; Mori et al., 2007). Not only do the compositions of complexes vary (i.e., binary KaiAC and KaiBC complexes and the ternary KaiABC complex), but subunit interactions undergo transformations as well, i.e., KaiC subunit shuffling (Kageyama et al., 2006; Mori et al., 2007) and KaiB tetramer to monomer conversion (Snijder et al., 2014; Villarreal et al., 2013). Moreover, the concentrations of individual Kai proteins and protein complexes oscillate over the daily period (Akiyama et al., 2008; Mori et al., 2007), and the protein–protein interfaces for the KaiA:KaiC interaction (Mori et al., 2007; Pattanayek et al., 2006, 2011; Qin, Byrne, Mori, et al., 2010; Vakonakis & LiWang, 2004) and possibly for the KaiB:KaiC interaction (Chang et al., 2011, 2012; Egli, 2014; Mutoh, Nishimura, Yasui, Onai, & Ishiura, 2013; Pattanayek et al., 2008, 2013; Tseng et al., 2014) undergo changes as KaiC cycles from the hypo to the hyper and back to the hypophosphorylated states. Correlating the dynamic formation of heteromultimeric complexes with models of 3D structure determinations using a hybrid structural approach involving EM, NMR, SAXS, X-ray, and a host of auxiliary approaches has turned out to be a significant challenge. Using ns EM, four particle shapes could be differentiated, i.e., KaiC hexamer and the KaiAC, KaiBC, and KaiABC complexes (Mori et al., 2007). EM and SAXS have provided 3D models of three complexes between full-length Kai proteins, but the resolution limits (maximal 16 Å) have not allowed a detailed visualization of the protein–protein interfaces (Egli, 2014; Pattanayek et al., 2008, 2006, 2011). Cryo-EM has thus far not provided high-resolution images of Kai complexes, and it appears that X-ray crystallography and NMR are the methods of choice for gaining insight into the dynamic protein–protein interactions between KaiA, B, and C at atomic resolution. However, only crystallography may allow visualization at that level of complexes involving the KaiC hexamer, with NMR investigations providing useful insights into interactions between monomeric domains (Chang et al., 2011, 2012; Tseng et al., 2014). Beyond the structural realm, there remain other phenomena governing Kai clock protein interactions whose origin and mechanism remain to be explored, among them temperature compensation (Murakami et al., 2008; Terauchi et al., 2007), a fundamental property of all biological clocks (Dunlap, Loros, & DeCoursey, 2004).

Although I have attempted to be as inclusive as possible in terms of the overview presented here of structural and biophysical approaches deployed

to analyze the KaiABC PTO, there remain of course additional techniques that could prove useful in the dissection of clock structure and mechanism. The most quantitative approach for determining the thermodynamic properties of protein–protein interactions is isothermal titration calorimetry (ITC; Pierce, Raman, & Nall, 1999), as it can provide information regarding stoichiometry, enthalpy, entropy, and binding kinetics for interacting proteins in solution without the need to immobilize or label them. We have used ITC in a preliminary fashion to measure changes in stability of the KaiC hexamer as a consequence of point mutations, but ultimately relied on circular dichroism melting experiments to just extract melting temperatures (Egli et al., 2013). Chemical cross-linking and mass spectrometry (XL-MS) is a technique that can help identify proximate amino acids and define the binding interface of protein–protein complexes, but for some reason cross-linking approaches have not been reported for the Kai system. XL-MS is now becoming an integral part of the hybrid structural biology approach for the analysis of protein complexes (Herzog et al., 2012). Provided a suitable cross-linking agent can be found for a particular complex, e.g., by screening of various bifunctional molecules with linkers of various lengths and reactive end groups, SDS-PAGE of cross-linked complexes, followed by proteolytic digestion (trypsin) of products from gel bands, and mass-spectrometric analysis of crosslinked peptides (XL-MS) can then be used to map the protein–protein interface (Leitner et al., 2010; Young et al., 2000).

A further approach that can shed light on protein interactions, the degree of proximity between partners, conformational changes and dynamics is electron paramagnetic resonance spectroscopy (Hubbell, Gross, Langen, & Lietzow, 1998; Mchaourab, Steed, & Kazmier, 2011). The KaiC protein from *S. elongatus* features three cysteins that are all located in the C-terminal half of hexamer subunits. Because they appear to be tucked away and therefore less reactive to labeling with a spin probe, introduction of a Cys mutation could be used to attach a label site specifically, e.g., on the N- or C-terminal surface, to probe the possibility that KaiB can bind on either side of the hexamer (Chang et al., 2012; Egli, 2014; Pattanayek et al., 2008, 2013; Tseng et al., 2014). Further, labeling two Kai proteins could furnish distance information for docking of crystal structures inside EM densities or SAXS envelopes, although this could prove very challenging owing to the hexameric nature of KaiC that will give rise to multiple distance pairs or rather distance distributions because of the intrinsic, environment-dependent mobility of spin labels. A related approach,

site-directed spin labeling electron spin resonance analysis, was applied to track down a transient interaction between KaiA and KaiB (Mutoh et al., 2010).

Finally, it could be interesting to apply single-molecule biophysics, e.g., pulling experiments (Aubin-Tam, Olivares, Sauer, Baker, & Lang, 2011), toward a more in-depth investigation of the stability, dynamics, and mechanism of the KaiA:KaiC interaction. Single-molecule approaches can give information about heterogeneous kinetics of molecules in the population of molecules. For example, it is likely that the various KaiC hexamers in the population do not all behave exactly the same, but that is the assumption of most of the biochemical analyses to date. Thus, such experiments may yield the forces necessary to pull out the KaiC C-terminal tail and the unraveling of the A-loop, processes that appear to form the basis for KaiA to stimulate KaiC phosphorylation, and in which different KaiC hexamers (e.g., in different phosphorylation states) may exhibit different kinetics. Another approach that potentially applies single-molecule advantages with the visualization capability of EM is atomic force microscopy (AFM). AFM is high-resolution scanning probe microscopy, with resolutions demonstrated down to subnanometer levels. High-speed AFM has been used to great effect on proteins similar in size and shape to KaiC, e.g., F1-ATPase where rotary catalysis and conformational changes that proceed around the hexameric ring were demonstrated (Uchihashi, Lino, Ando, & Noji, 2011).

ACKNOWLEDGMENTS

This work is supported in part by NIH Grant R01 GM073845. I am grateful to Dr. Carl H. Johnson, Vanderbilt University, for many years of a fruitful collaboration between our labs on research directed at the structure and function of the cyanobacterial circadian clock, insights regarding applications of fluorescence anisotropy and FRET as well as mathematical modeling to studies of the KaiABC oscillator and for helpful comments on the manuscript.

REFERENCES

Akiyama, S., Nohara, A., Ito, K., & Maeda, Y. (2008). Assembly and disassembly dynamics of the cyanobacterial periodosome. *Molecular Cell*, *29*, 703–716.

Amunts, A., Brown, A., Bai, X., Llacer, J. L., Hussain, T., Emsley, P., et al. (2014). Structure of the yeast mitochondrial large ribosomomal subunit. *Nature*, *343*, 1485–1489.

Aubin-Tam, M.-E., Olivares, A. O., Sauer, R. T., Baker, T. A., & Lang, M. J. (2011). Single-molecule protein unfolding and translocation by an ATP-fueled proteolytic machine. *Cell*, *145*, 257–267.

Berendsen, H. J. C., Grigera, J. R., & Straatsma, T. P. (1987). The missing term in effective pair potentials. *Journal of Physical Chemistry*, *91*, 6269–6271.

Brettschneider, C., Rose, R. J., Hertel, S., Axmann, I. M., Heck, A. J., & Kollmann, M. (2010). A sequestration feedback determines dynamics and temperature entrainment of the KaiABC circadian clock. *Molecular Systems Biology*, *6*, 389.

Byrne, M. (2009). Mathematical modeling of the in vitro cyanobacterial circadian oscillator. In J. L. Ditty, S. R. Mackey, & C. H. Johnson (Eds.), *Bacterial circadian programs: Vol. 16.* (pp. 283–300). Berlin: Springer Publishers.

Case, D. A., Darden, T. A., Cheatham, T. E., III, Simmerling, C. L., Wang, J., Duke, R. E., et al. (2012). *AMBER 12.* San Francisco: University of California.

Chang, Y. G., Kuo, N. W., Tseng, R., & LiWang, A. (2011). Flexibility of the C-terminal, or CII, ring of KaiC governs the rhythm of the circadian clock of cyanobacteria. *Proceedings of the National Academy of Sciences of the United States of America*, *108*, 14431–14436.

Chang, Y. G., Tseng, R., Kuo, N. W., & LiWang, A. (2012). Rhythmic ring-ring stacking drives the circadian oscillator clockwise. *Proceedings of the National Academy of Sciences of the United States of America*, *109*, 16847–16851.

Clodong, S., Düring, U., Kronk, L., Axmann, I., Wilde, A., Herzel, H., et al. (2007). Functioning and robustness of a bacterial circadian clock. *Molecular Systems Biology*, *3*, 90.

Czarna, A., Berndt, A., Singh, H. R., Grudziecki, A., Ladurner, A. G., Timinszky, G., et al. (2013). Structures of *Drosophila* cryptochrome and mouse cryptochrome1 provide insight into circadian function. *Cell*, *153*, 1394–1405.

Dominguez, C., Boelens, R., & Bonvin, A. M. J. J. (2003). HADDOCK: A protein–protein docking approach based on biochemical and/or biophysical information. *Journal of the American Chemical Society*, *125*, 1731–1737.

Dunlap, J. C., Loros, J. J., & DeCoursey, P. J. (Eds.). (2004). *Chronobiology: Biological timekeeping*. Sunderland, MA: Sinauer Associates, Inc., Publishers.

Durrant, J. D., & McCammon, J. A. (2011). Molecular dynamics simulations and drug discovery. *BMC Biology*, *9*, 71–79.

Egli, M. (2010). Diffraction techniques in structural biology. *Current Protocols in Nucleic Acid Chemistry*, *41*, 7.13.1–7.13.35.

Egli, M. (2014). Intricate protein–protein interactions in the cyanobacterial circadian clock. *Journal of Biological Chemistry*, *289*, 21267–21275.

Egli, M., & Johnson, C. H. (2013). A circadian clock nanomachine that runs without transcription or translation. *Current Opinion in Neurobiology*, *23*, 732–740.

Egli, M., Mori, T., Pattanayek, R., Xu, Y., Qin, X., & Johnson, C. H. (2012). Dephosphorylation of the core clock protein KaiC in the cyanobacterial KaiABC circadian oscillator proceeds via an ATP synthase mechanism. *Biochemistry*, *51*, 1547–1558.

Egli, M., Pattanayek, R., Sheehan, J. H., Xu, Y., Mori, T., Smith, J. A., et al. (2013). Loop–loop interactions regulate KaiA-stimulated KaiC phosphorylation in the cyanobacterial KaiABC circadian clock. *Biochemistry*, *52*, 1208–1220.

Emberly, E., & Wingreen, N. S. (2006). Hourglass model for a protein-based circadian oscillator. *Physical Reviews Letters*, *96*, 0383003.

Englander, S. W., & Kallenbach, N. R. (1983). Hydrogen exchange and structural dynamics of proteins and nucleic acids. *Quarterly Reviews of Biophysics*, *16*, 521–655.

Garces, R. G., Wu, N., Gillon, W., & Pai, E. F. (2004). Anabaena circadian clock proteins KaiA and KaiB reveal potential common binding site to their partner KaiC. *EMBO Journal*, *23*, 1688–1698.

Götz, A. W., Williamson, M. J., Xu, D., Poole, D., Le Grand, S., & Walker, R. C. (2012). Routine microsecond molecular dynamics simulations with AMBER on GPUs. 1. Generalized born. *Journal of Chemical Theory and Computation*, *8*, 1542–1555.

Harp, J. M., Hanson, B. F., Timm, D. E., & Bunick, G. J. (1999). Macromolecular crystal annealing: Evaluation of techniques and variables. *Acta Crystallographica Section D*, *55*, 1329–1334.

Hayashi, F., Ito, H., Fujita, M., Iwase, R., Uzumaki, T., & Ishiura, M. (2004). Stoichiometric interactions between cyanobacterial clock proteins KaiA and KaiC. *Biochemical and Biophysical Research Communications*, *316*, 195–202.

Hayashi, F., Iwase, R., Uzumaki, T., & Ishiura, M. (2006). Hexamerization by the N-terminal domain and intersubunit phosphorylation by the C-terminal domain of cyanobacterial circadian clock protein KaiC. *Biochemical and Biophysical Research Communications*, *318*, 864–872.

Hayashi, F., Suzuki, H., Iwase, R., Uzumaki, T., Miyake, A., Shen, J.-R., et al. (2003). ATP-induced hexameric ring structure of the cyanobacterial circadian clock protein KaiC. *Genes to Cells*, *8*, 287–296.

Hellweger, F. L. (2010). Resonating circadian clocks enhance fitness in cyanobacteria *in silico*. *Ecological Modelling*, *221*, 1620–1629.

Hennig, S., Strauss, H. M., Vanselow, K., Yildiz, O., Schulze, S., Arens, J., et al. (2009). Structural and functional analyses of PAS domain interactions of the clock proteins Drosophila PERIOD and mouse PERIOD2. *PLoS Biology*, *7*, e94.

Herzog, F., Kahraman, A., Boehringer, D., Mak, R., Bracher, A., Walzthoeni, T., et al. (2012). Structural probing of a protein phosphatase 2A network by chemical crosslinking and mass spectrometry. *Science*, *337*, 1348–1352.

Hitomi, K., Oyama, T., Han, S., Arvai, A. S., & Getzoff, E. D. (2005). Tetrameric architecture of the circadian clock protein KaiB: A novel interface for intermolecular interactions and its impact on the circadian rhythm. *Journal of Biological Chemistry*, *280*, 18643–18650.

Huang, N., Chelliah, Y., Shan, Y., Taylor, C. A., Yoo, S.-H., Partch, C., et al. (2012). Crystal structure of the heterodimeric CLOCK:BMAL1 transcriptional activator complex. *Science*, *337*, 189–194.

Hubbell, W. L., Gross, A., Langen, R., & Lietzow, M. A. (1998). Recent advances in site-directed spin labeling of protein. *Current Opinion in Structural Biology*, *8*, 649–656.

Ishiura, M., Kutsuna, S., Aoki, S., Iwasaki, H., Andersson, C. R., Tanabe, A., et al. (1998). Expression of a gene cluster *kaiABC* as a circadian feedback process in cyanobacteria. *Science*, *281*, 1519–1523.

Ito, H., Kageyama, H., Mutsuda, M., Nakajima, M., Oyama, T., & Kondo, T. (2007). Autonomous synchronization of the circadian KaiC phosphorylation rhythm. *Nature Structural and Molecular Biology*, *14*, 1084–1088.

Iwasaki, H., Nishiwaki, T., Kitayama, Y., Nakajima, M., & Kondo, T. (2002). KaiA-stimulated KaiC phosphorylation in circadian timing loops in cyanobacteria. *Proceedings of the National Academy of Sciences of the United States of America*, *99*, 15788–15793.

Iwase, R., Imada, K., Hayashi, F., Uzumaki, T., Morishita, M., Onai, K., et al. (2005). Functionally important substructures of circadian clock protein KaiB in a unique tetramer complex. *Journal of Biological Chemistry*, *280*, 43141–43149.

Jacrot, B. (1976). The study of biological structures by neutron scattering from solution. *Reports on Progress in Physics*, *39*, 911–953.

Johnson, C. H., Egli, M., & Stewart, P. L. (2008). Structural insights into a circadian oscillator. *Science*, *322*, 697–701.

Johnson, C. H., Stewart, P. L., & Egli, M. (2011). The cyanobacterial circadian system: From biophysics to bioevolution. *Annual Review of Biophysics*, *40*, 143–167.

Kageyama, H., Nishiwaki, T., Nakajima, M., Iwasaki, H., Oyama, T., & Kondo, T. (2006). Cyanobacterial circadian pacemaker: Kai protein complex dynamics in the KaiC phosphorylation cycle *in vitro*. *Molecular Cell*, *23*, 161–171.

Katta, V., & Chait, B. T. (1991). Conformational changes in proteins probed by hydrogen-exchange electrospray-ionization mass spectrometry. *Rapid Communications in Mass Spectrometry*, *5*, 214–217.

Keeler, J. (2005). *Understanding NMR* (1st ed.). Hoboken, NJ: John Wiley & Sons.

Kim, Y. I., Dong, G., Carruthers, C. W., Jr., Golden, S. S., & LiWang, A. (2008). The day/night switch in KaiC, a central oscillator component of the circadian clock of cyanobacteria. *Proceedings of the National Academy of Sciences of the United States of America*, *105*, 12825–12830.

Kitayama, Y., Iwasaki, H., Nishiwaki, T., & Kondo, T. (2003). KaiB functions as an attenuator of KaiC phosphorylation in the cyanobacterial circadian clock system. *EMBO Journal*, *22*, 1–8.

Kitayama, K., Nishiwaki-Ohkawa, T., Sugisawa, Y., & Kondo, T. (2014). KaiC intersubunit communication facilitates robustness of circadian rhythms in cyanobacteria. *Nature Communications*, *4*, 3897.

Konermann, L., Pan, J., & Liu, Y. H. (2011). Hydrogen exchange mass spectrometry for studying protein structure and dynamics. *Chemical Society Reviews*, *40*, 1223–1234.

Kucera, N., Schmalen, I., Hennig, S., Ölliger, R., Strauss, H. M., Grudziecki, A., et al. (2012). Unwinding the differences of the mammalian PERIOD clock proteins from crystal structure to cellular function. *Proceedings of the National Academy of Sciences of the United States of America*, *109*, 3311–3316.

Kurosawa, G., Aihara, K., & Iwasa, Y. (2006). A model for the circadian rhythm of cyanobacteria that maintains oscillation without gene expression. *Biophysical Journal*, *91*, 2015–2023.

Leipe, D. D., Aravind, L., Grishin, N. V., & Koonin, E. V. (2000). The bacterial replicative helicase DnaB evolved from a RecA duplication. *Genome Research*, *10*, 5–16.

Leitner, A., Walzthoeni, T., Kahraman, A., Herzog, F., Rinner, O., Beck, M., et al. (2010). Probing native protein structures by chemical cross-linking, mass spectrometry, and bioinformatics. *Molecular and Cellular Proteomics*, *9*, 1634–1649.

Li, C., Chen, X., Wang, P., & Wang, W. (2009). Circadian KaiC phosphorylation: A multilayer network. *PLoS Computational Biology*, *5*, e1000568.

Li, S., & Fang, Y. H. (2007). Modelling circadian rhythms of protein KaiA, KaiB and KaiC interactions in cyanobacteria. *Biological Rhythm Research*, *38*, 43–53.

Ma, L., & Ranganathan, R. (2012). Quantifying the rhythm of KaiB–C interaction for in vitro cyanobacterial circadian clock. *PLoS One*, *7*, e42581.

Mandell, J. G., Baerga-Ortiz, A., Falick, A. M., & Komives, E. A. (2005). Measurement of solvent accessibility at protein–protein interfaces. *Methods in Molecular Biology*, *305*, 65–80.

Markson, J. S., Piechura, J. R., Puszynska, A. M., & O'Shea, E. K. (2013). Circadian control of global gene expression by the cyanobacterial master regulator RpaA. *Cell*, *155*, 1396–1408.

Mchaourab, H. S., Steed, P. R., & Kazmier, K. (2011). Toward the fourth dimension of membrane protein structure: Insights into dynamics from spin-labeling EPR spectroscopy. *Structure*, *19*, 1549–1561.

Meagher, K. L., Redman, L. T., & Carlson, H. A. (2003). Development of polyphosphate parameters for use with the AMBER force field. *Journal of Computational Chemistry*, *24*, 1016–1025.

Mehra, A., Hong, C., Shi, M., Loros, J., Dunlap, J., & Ruoff, P. (2006). Circadian rhythmicity by autocatalysis. *PLoS Computational Biology*, *2*, e96.

Meilleur, F., Weiss, K. L., & Myles, D. A. A. (2009). Deuterium labeling for neutron structure–function–dynamics analysis. *Methods in Molecular Biology*, *544*, 281–292.

Miyoshi, F., Nakayama, Y., Kaizu, K., Iwasaki, H., & Tomita, M. (2007). A mathematical model for the Kai-protein-based chemical oscillator and clock gene expression rhythms in cyanobacteria. *Journal of Biological Rhythms*, *22*, 69–80.

Mori, T., Saveliev, S. V., Xu, Y., Stafford, W. F., Cox, M. M., Inman, R. B., et al. (2002). Circadian clock protein KaiC forms ATP-dependent hexameric rings and binds DNA. *Proceedings of the National Academy of Sciences of the United States of America*, *99*, 17203–17208.

Mori, T., Williams, D. R., Byrne, M. O., Qin, X., Egli, M., McHaourab, H. S., et al. (2007). Elucidating the ticking of an *in vitro* circadian clockwork. *PLoS Biology*, *5*, e93.

Murakami, R., Miyake, A., Iwase, R., Hayashi, F., Uzumaki, T., & Ishiura, M. (2008). ATPase activity and its temperature compensation of the cyanobacterial clock protein KaiC. *Genes to Cells*, *13*, 387–395.

Murayama, Y., Mukaiyama, A., Imai, K., Onoue, Y., Tsunoda, A., Nohara, A., et al. (2011). Tracking and visualizing the circadian ticking of the cyanobacterial clock protein KaiC in solution. *EMBO J*, *30*, 68–78.

Mutoh, R., Mino, H., Murakami, R., Uzumaki, T., Takabayashi, A., Ishii, K., et al. (2010). Direct interaction between KaiA and KaiB revealed by a site-directed spin labeling electron spin resonance analysis. *Genes to Cells*, *15*, 269–280.

Mutoh, R., Nishimura, A., Yasui, S., Onai, K., & Ishiura, M. (2013). The ATP-mediated regulation of KaiB–KaiC interaction in the cyanobacterial circadian clock. *PLoS One*, *8*, e80200.

Nagai, T., Terada, T. P., & Sasai, M. (2010). Synchronization of circadian oscillation of phosphorylation level of KaiC in vitro. *Biophysical Journal*, *98*, 2469–2477.

Nakajima, M., Imai, K., Ito, H., Nishiwaki, T., Murayama, Y., Iwasaki, H., et al. (2005). Reconstitution of circadian oscillation of cyanobacterial KaiC phosphorylation in vitro. *Science*, *308*, 414–415.

Nishiwaki, T., & Kondo, T. (2012). Circadian autodephosphorylation of cyanobacterial clock protein KaiC occurs via formation of ATP as intermediate. *Journal of Biological Chemistry*, *287*, 18030–18035.

Nishiwaki, T., Satomi, Y., Kitayama, Y., Terauchi, K., Kiyohara, R., Takao, T., et al. (2007). A sequential program of dual phosphorylation of KaiC as a basis for circadian rhythm in cyanobacteria. *EMBO Journal*, *26*, 4029–4037.

Nishiwaki, T., Satomi, Y., Nakajima, M., Lee, C., Kiyohara, R., Kageyama, H., et al. (2004). Role of KaiC phosphorylation in the circadian clock system of Synechococcus elongatus PCC 7942. *Proceedings of the National Academy of Sciences of the United States of America*, *101*, 13927–13932.

Paddock, M. L., Boyd, J. S., Adin, D. M., & Golden, S. S. (2013). Active output state of the Synechococcus Kai circadian oscillator. *Proceedings of the National Academy of Sciences of the United States of America*, *110*, E3849–E3857.

Pattanayek, R., Mori, T., Xu, Y., Pattanayek, S., Johnson, C. H., & Egli, M. (2009). Structures of KaiC circadian clock mutant proteins: A new phosphorylation site at T426 and mechanisms of kinase, ATPase and phosphatase. *PLoS One*, *4*, e7529.

Pattanayek, R., Sidiqi, S. K., & Egli, M. (2012). Crystal structure of the redox-active cofactor DBMIB bound to circadian clock protein KaiA and structural basis for DBMIB's ability to prevent stimulation of KaiC phosphorylation by KaiA. *Biochemistry*, *51*, 8050–8052.

Pattanayek, R., Wang, J., Mori, T., Xu, Y., Johnson, C. H., & Egli, M. (2004). Visualizing a circadian clock protein: Crystal structure of KaiC and functional insights. *Molecular Cell*, *15*, 375–388.

Pattanayek, R., Williams, D. R., Pattanayek, S., Mori, T., Johnson, C. H., Stewart, P. L., et al. (2008). Structural model of the circadian clock KaiB–KaiC complex and mechanism for modulation of KaiC phosphorylation. *EMBO Journal*, *27*, 1767–1778.

Pattanayek, R., Williams, D. R., Pattanayek, S., Xu, Y., Mori, T., Johnson, C. H., et al. (2006). Analysis of KaiA–KaiC protein interactions in the cyano-bacterial circadian clock using hybrid structural methods. *EMBO Journal*, *25*, 2017–2028.

Pattanayek, R., Williams, D. R., Rossi, G., Weigand, S., Mori, T., Johnson, C. H., et al. (2011). Combined SAXS/EM based models of the S. elongatus post-translational circadian oscillator and its interactions with the output His-kinase SasA. *PLoS One*, *6*, e23697.

Pattanayek, R., Xu, Y., Lamichhane, A., Johnson, C. H., & Egli, M. (2014). An arginine tetrad as mediator of input-dependent and input-independent ATPases in the clock protein KaiC. *Acta Crystallographica Section D*, *70*, 1375–1390.

Pattanayek, R., Yadagirib, K. K., Ohi, M. D., & Egli, M. (2013). Nature of KaiB–KaiC binding in the cyanobacterial circadian oscillator. *Cell Cycle*, *12*, 810–817.

Petoukhov, M. V., & Svergun, D. I. (2005). Global rigid body modeling of macromolecular complexes against small-angle scattering data. *Biophysical Journal*, *89*, 1237–1250.

Phong, C., Markson, J. S., Wilhoite, C. M., & Rust, M. J. (2013). Robust and tunable circadian rhythms from differentially sensitive catalytic domains. *Proceedings of the National Academy of Sciences of the United States of America*, *110*, 1124–1129.

Pierce, M. M., Raman, C. S., & Nall, B. T. (1999). Isothermal titration calorimetry of protein–protein interactions. *Methods*, *19*, 213–221.

Putnam, C. D., Hammel, M., Hura, G. L., & Tainer, J. A. (2007). X-ray solution scattering (SAXS) combined with crystallography and computation: Defining accurate macromolecular structures, conformations and assemblies in solution. *Quarterly Reviews of Biophysics*, *40*, 191–285.

Qin, X., Byrne, M., Mori, T., Zou, P., Williams, D. R., Mchaourab, H., et al. (2010). Intermolecular associations determine the dynamics of the circadian KaiABC oscillator. *Proceedings of the National Academy of Sciences of the United States of America*, *107*, 14805–14810.

Qin, X., Byrne, M., Xu, Y., Mori, T., & Johnson, C. H. (2010). Coupling of a core post-translational pacemaker to a slave transcription/translation feedback loop in a circadian system. *PLoS Biology*, *8*, e1000394.

Rambo, R. P., & Tainer, J. A. (2013). Accurate assessment of mass, models and resolution by small-angle scattering. *Nature*, *496*, 477–481.

Reddy, V. S., Natchiar, S. K., Stewart, P. L., & Nemerow, G. R. (2010). Crystal structure of human adenovirus at 3.5 Å resolution. *Science*, *329*, 1071–1075.

Rust, M. J., Golden, S. S., & O'Shea, E. K. (2011). Light-driven changes in energy metabolism directly entrain the cyanobacterial circadian oscillator. *Science*, *331*, 220–223.

Rust, M. J., Markson, J. S., Lane, W. S., Fisher, D. S., & O'Shea, E. K. (2007). Ordered phosphorylation governs oscillation of a three-protein circadian clock. *Science*, *318*, 809–812.

Schmalen, I., Reischl, S., Wallach, T., Klemz, R., Grudziecki, A., Prabu, J. R., et al. (2014). Interaction of circadian clock proteins CRY1 and PER2 is modulated by zinc binding and disulfide bond formation. *Cell*, *157*, 1203–1215.

Schwede, T., & Peitsch, M. C. (Eds.). (2008). *Computational structural biology: Methods and applications*. Hackensack, NJ: World Scientific Publishing Co.

Snijder, J., Burnley, R. J., Wiegard, A., Melquiond, A. S. J., Bonvin, A. M. J. J., Axmann, I. M., et al. (2014). Insight into cyanobacterial circadian timing from structural details of the KaiB–KaiC interaction. *Proceedings of the National Academy of Sciences of the United States of America*, *111*, 1379–1384.

Takigawa-Imamura, H., & Mochizuki, A. (2006). Predicting regulation of the phosphorylation cycle of KaiC clock protein using mathematical analysis. *Journal of Biological Rhythms*, *21*, 405–416.

Teng, S. W., Mukherij, S., Moffitt, J. R., de Buyl, S., & O'Shea, E. K. (2013). Robust circadian oscillations in growing cyanobacteria require transcriptional feedback. *Science*, *340*, 737–740.

Terauchi, K., Kitayama, Y., Nishiwaki, T., Miwa, K., Murayama, Y., Oyama, T., et al. (2007). The ATPase activity of KaiC determines the basic timing for circadian clock of cyanobacteria. *Proceedings of the National Academy of Sciences of the United States of America*, *104*, 16377–16381.

Trabuco, L. G., Villa, E., Schreiner, E., Harrison, C. B., & Schulten, K. (2009). Molecular dynamics flexible fitting: A practical guide to combine cryo-electron microscopy and X-ray crystallography. *Methods*, *49*, 174–180.

Tseng, R., Chang, Y.-G., Bravo, I., Latham, R., Chaudhary, A., Kuo, N.-W., et al. (2014). Cooperative KaiA–KaiB–KaiC interactions affect KaiB/SasA competition in the circadian clock of cyanobacteria. *Journal of Molecular Biology*, *426*, 389–402.

Uchihashi, T., Lino, R., Ando, T., & Noji, H. (2011). High-speed atomic force microscopy reveals rotary catalysis of rotorless F1-ATPase. *Science*, *333*, 755–758.

Vakonakis, I., Klewer, D. A., Williams, S. B., Golden, S. S., & LiWang, A. C. (2004). Structure of the N-terminal domain of the circadian clock-associated histidine kinase SasA. *Journal of Molecular Biology*, *342*, 9–17.

Vakonakis, I., & LiWang, A. C. (2004). Structure of the C-terminal domain of the clock protein KaiA in complex with a KaiC-derived peptide: Implications for KaiC regulation. *Proceedings of the National Academy of Sciences of the United States of America*, *101*, 10925–10930.

van Duijn, E. (2010). Current limitations in native mass spectrometry based structural biology. *Journal of the American Society for Mass Spectrometry*, *21*, 971–978.

van Zon, J. S., Lubensky, D. K., Altena, P. R., & ten Wolde, P. R. (2007). An allosteric model of circadian KaiC phosphorylation. *Proceedings of the National Academy of Sciences of the United States of America*, *104*, 7420–7425.

Villarreal, S. A., Pattanayek, R., Williams, D. R., Mori, T., Qin, X., Johnson, C. H., et al. (2013). CryoEM and molecular dynamics of the circadian KaiB–KaiC complex indicates KaiB monomers interact with KaiC and block ATP binding clefts. *Journal of Molecular Biology*, *425*, 3311–3324.

Volkov, V. V., & Svergun, D. I. (2003). Uniqueness of ab initio shape determination in small-angle scattering. *Journal of Applied Crystallography*, *36*, 860–864.

Wales, T. E., & Engen, J. R. (2006). Hydrogen exchange mass spectrometry for the analysis of protein dynamics. *Mass Spectrometry Reviews*, *25*, 158–170.

Wang, J., Xu, L., & Wang, E. (2009). Robustness and coherence of a three-protein circadian oscillator: Landscape and flux perspectives. *Biophysical Journal*, *97*, 3038–3046.

Whitten, A. E., Cai, S., & Trewhella, J. (2008). MULCh: Modules for the analysis of small-angle neutron contrast variation data from biomolecular assemblies. *Journal of Applied Crystallography*, *41*, 222–226.

Williams, S. B., Vakonakis, I., Golden, S. S., & LiWang, A. C. (2002). Structure and function from the circadian clock protein KaiA of *Synechococcus elongatus*: A potential clock input mechanism. *Proceedings of the National Academy of Sciences of the United States of America*, *99*, 15357–15362.

Wood, T. L., Bridwell-Rabb, J., Kim, Y.-I., Gao, T., Chang, Y.-G., LiWang, A., et al. (2010). The KaiA protein of the cyanobacterial circadian oscillator is modulated by a redox-active cofactor. *Proceedings of the National Academy of Sciences of the United States of America*, *107*, 5804–5809.

Wüthrich, K. (1986). *NMR of proteins and nucleic acids* (1st ed.). New York: John Wiley & Sons.

Xu, Y., Mori, T., & Johnson, C. H. (2003). Cyanobacterial circadian clockwork: Roles of KaiA, KaiB, and the kaiBC promoter in regulating KaiC. *EMBO Journal*, *22*, 2117–2126.

Xu, Y., Mori, T., Pattanayek, R., Pattanayek, S., Egli, M., & Johnson, C. H. (2004). Identification of key phosphorylation sites in the circadian clock protein KaiC by crystallographic and mutagenetic analyses. *Proceedings of the National Academy of Sciences of the United States of America*, *101*, 13933–13938.

Xu, Y., Mori, T., Qin, X., Yan, H., Egli, M., & Johnson, C. H. (2009). Intramolecular regulation of phosphorylation status of the circadian clock protein KaiC. *PLoS One*, *4*, e7509.

Yang, Q., Pando, B. F., Dong, G., Golden, S. S., & van Oudenaarden, A. (2010). Circadian gating of the cell cycle revealed in single cyanobacterial cells. *Science*, *327*, 1522–1526.
Ye, S., Vakonakis, I., Ioerger, T. R., LiWang, A. C., & Sacchettini, J. C. (2004). Crystal structure of circadian clock protein KaiA from *Synechococcus elongatus*. *Journal of Biological Chemistry*, *279*, 20511–20518.
Yoda, M., Eguchi, K., Terada, T. P., & Sasai, M. (2007). Monomer-shuffling and allosteric transition in KaiC circadian oscillation. *PLoS One*, *2*, e408.
Young, M. M., Tang, N., Hempel, J. C., Oshiro, C. M., Taylor, E. W., Kuntz, I. D., et al. (2000). High throughput protein fold identification by using experimental constraints derived from intramolecular cross-links and mass spectrometry. *Proceedings of the National Academy of Sciences of the United States of America*, *97*, 5802–5806.
Zoltowski, B. D., Vaidya, A. T., Top, D., Widom, J., Young, M. W., & Crane, B. R. (2011). Structure of full-length Drosophila cryptochrome. *Nature*, *480*, 396–400.
Zwicker, D., Lubensky, D. K., & ten Wolde, P. R. (2010). Robust circadian clocks from coupled protein-modification and transcription-translation cycles. *Proceedings of the National Academy of Sciences of the United States of America*, *107*, 22540–22545.